## Graphical Abstract

**Novel Epidithiodiketopiperazines as anti-viral zinc ejectors of the Feline Immunodeficiency Virus (FIV) nucleocapsid protein as a model for HIV infection**

Christopher R. M. Asquith, Bruno C. Sil, Tuomo Laitinen, Graham J. Tizzard, Simon J. Coles, Antti Poso, Regina Hofmann-Lehmann, Stephen T. Hilton

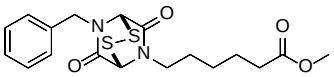


**Compound 42**
CrFK - 100% vaiblity at 10 μM
FL-4 - $CC_{50}$ = >10 μM
FL-4 - $EC_{50}$ = 0.034 μM
TI - >300

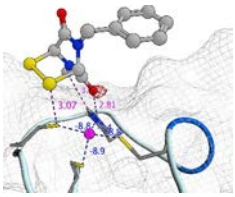

# Novel Epidithiodiketopiperazines as anti-viral zinc ejectors of the Feline Immunodeficiency Virus (FIV) nucleocapsid protein as a model for HIV infection

Christopher R. M. Asquith[a,b,c,*], Bruno C. Sil[a,d], Tuomo Laitinen[e], Graham J. Tizzard[f], Simon J. Coles[f], Antti Poso[e], Regina Hofmann-Lehmann[b], Stephen T. Hilton[a,*]

[a]*School of Pharmacy, Faculty of Life Sciences, University College London, London, WC1N 1AX, United Kingdom*
[b]*Clinical Laboratory & Center for Clinical Studies, Vetsuisse Faculty, University of Zurich, 8057 Zurich, Switzerland.*
[c]*Department of Pharmacology, School of Medicine, University of North Carolina at Chapel Hill, Chapel Hill, NC 27599, USA*
[d]*School of Human Sciences, London Metropolitan University, 166-220 Holloway Road, London, N7 8DB, United Kingdom.*
[e]*School of Pharmacy, Faculty of Health Sciences, University of Eastern Finland, Kuopio, 70211, Finland.*
[f]*UK National Crystallography Service, School of Chemistry, University of Southampton, Highfield Campus, Southampton, SO17 1BJ, United Kingdom.*

ABSTRACT

Focused libraries of multi-substituted epidithiodiketopiperazines (ETP) were prepared and evaluated for efficacy of inhibiting the nucleocapsid protein function of the Feline Immunodeficiency Virus (FIV) as a model for HIV. This activity was compared and contrasted to observed toxicity utilizing an *in-vitro* cell culture approach. This resulted in the identification of several promising lead compounds with nanomolar potency in cells with low toxicity and a favourable therapeutic index.

## Introduction

There are multiple inhibition targets and inhibitors of the Human Immunodeficiency Virus (HIV) highlighting the challenge posed by this constantly evolving disease.[1] The ability of the virus to mutate and maintain function is key to its continued virulence. This has resulted in over 25 million Acquired Immune Deficiency Syndrome (AIDS) related deaths worldwide; with over 34 million people currently suffering from the HIV.[2]

The domestic cat is an effective non-primate animal model for lentivirus infections.[3] The feline model is the smallest natural host for a lentiviral infection with an acute phase and a variable latent phase.[3b] Feline Immunodeficiency Virus (FIV) has an analogous AIDS type progression with neurological involvement and selective CD4+ lymphocyte depletion.[4] FIV was the first lentivirus to demonstrate resistance,[5] which is a key obstacle in the effective treatment of HIV.[6] One way to combat this issue would be to target mutation resistant proteins at the core of the viral replication cycle. The double zinc finger nucleocapsid protein (NCp) fits this profile, with involvement at multiple points of the viral replication cycle where deletion or modification of either zinc finger leads to virus inactivation.[7]

* Corresponding authors. E-mail address: chris.asquith@unc.edu (C. R. M. Asquith) and s.hilton@ucl.ac.uk (S.T. Hilton).

The NCp has multiple roles within the viral replication cycle including packing, dimerization, organization of the protein-RNA complexes within the newly created virons and annealing of the cellular primer $^{t}RNA3^{lys}$ to the primer binding site in reverse transcriptase.[7] The NCp double zinc finger peptide unit C-$X_2$-C-$X_4$-H-$X_4$-C (CCHC) is conserved across almost all retroviruses including HIV-1/2, FIV, Simian Immunodeficiency Virus (SIV), Equine Infectious Anemia Virus (EIAV) and others.[8]

Despite the promising potential of targeting the NCp there are currently no clinically approved small molecule inhibitors.[9-10] While there have been several recent examples of protein binders to the nucleic acid binding cleft between the two zinc fingers with some encouraging results none have progressed to the clinic.[11] However, there are two high profile zinc ejectors that have been used clinically. The first, was azodicarbonamide (ADA) - **1** an anti-viral zinc ejector progressed to phase 1/2 clinical trials but was later withdrawn.[12] The other was a benzisothiazolone (BITA) - **2** zinc ejector that also failed to reach the progression milestones.[13] These are part of a wider suite of compounds that have been shown to be activity *via* zinc ejection (**Figure 1**). These include the original zinc ejectors 3-nitrosobenzamide (NOBA) - **3** and 2,2'-di-thiobisbenzamide (DIBA) - **4**, with more recent examples including 2,2-diselenobisbenzamides (DISeBAs) - **5** and pyridinioalkanoyl thiolesters (PATES) - **6** among others.[12-14]

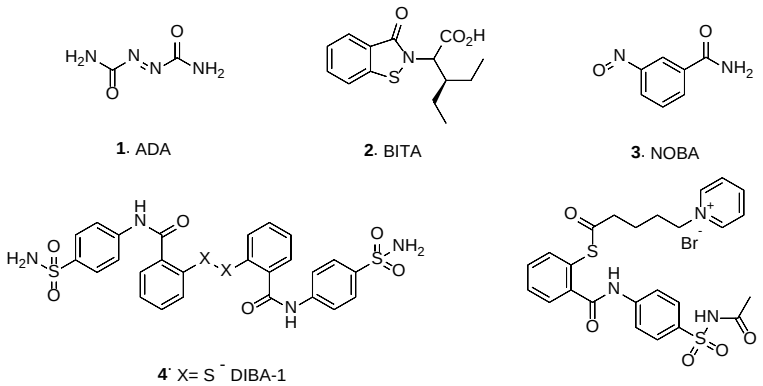


**Figure 1**. Examples of some significant previously reported zinc ejectors

The zinc ejection mechanism has demonstrated potential on a number of biological applications including metallothionein for oxidative stress,[15] transcription factors involved in viral replication[16] and inhibition of histone lysine demethylase JMJD2A.[17] The HIF-1 alpha/P300 interaction triple zinc finger has also been effectively targeted with a number of different chemotypes.[18] One of these chemotypes is the epidithiodiketopiperazine (ETP) which has a known internal redox chemistry and an ability to coordinate zinc.[18a,19]

A diverse portfolio of biological activities including anti-viral, anti-bacterial and immunomodulation have been demonstrated by the ETP class of compound. This has resulted in the ETP core being the focus of many synthetic efforts and structural elucidations (**6**-**14**).[20] The ETP natural products (**Figure 2**) have historically been difficult to synthesize due to the complex structure and the sensitivity of the disulfide bond.[20]

## Results and Discussion

Most reported synthetic approaches towards the ETP core have relied on formation of the diketopiperazine ring prior to addition of sulfur either *via* displacement of a leaving group, or addition of sulfur to an intermediate iminium ion.[21,20q,20y] Recent approaches have shown that simple ETP derivatives can be obtained by reaction of the diketopiperazine ring with sulfur or sulfur electrophiles under basic conditions.[22,20k] We utilized a hybrid approach where the diketopiperazine ring is formed at the same time as sulfur is incorporated (**Scheme 1**).[23] This reduced the overall number of steps required to access the ETP core and mitigated some of the functionality issues associated with late stage addition of sulfur.

First benzylamine (**15**) or methylamine (**16**) was added to a solution of ethyl glyoxalate in toluene, followed by the addition of *p*-methoxybenzylmercaptan to form **17** and **18** using the Dean and Stark method, in high yield. This was followed by coupling of 2-chloro-2-oxoethane-1,1-diyl diacetate to form diacetate intermediates **19** and **20**.[23a] The cyclisation precursor **19** and **20** were then treated with *p*-methoxybenzylmercaptan and the corresponding amine (**Table 1**) with a 4-dimethylaminopyridine (DMAP) catalysis to produce **21-32** which were set up in the correct orientation to form the disulfide bridge motif. The *p*-methoxybenzyl (PMB) protecting groups were cleaved with boron tribromide at -78 °C, before being warmed and treated with iodine to furnish the final ETP core **33-44** in good to excellent yields (**Scheme 1**).

The compounds (**33**-**44**) were initially tested at three higher concentrations (100, 10 & 1 μM) in a MTT cell viability assay over 24 hours using Crandell Rees Feline Kidney (CrFK) cells as a measurement of acute toxcity.[24,25] These initial results highlighted compounds that were acutely toxic (**Table 1**). The compounds (**33**-**44**) were then tested for anti-viral capabilities against FIV using an IL-2 independent feline lymphoblastoid (FL-4) cell at six concentrations (100 μM - 1 nM) over a period of seven days.[25,26] These chronically infected FL-4 cells were exposed to **33**-**44** over a period of seven days and sampled every day at each of six concentrations to determine the extent of viral replication/viral suppression.[25]

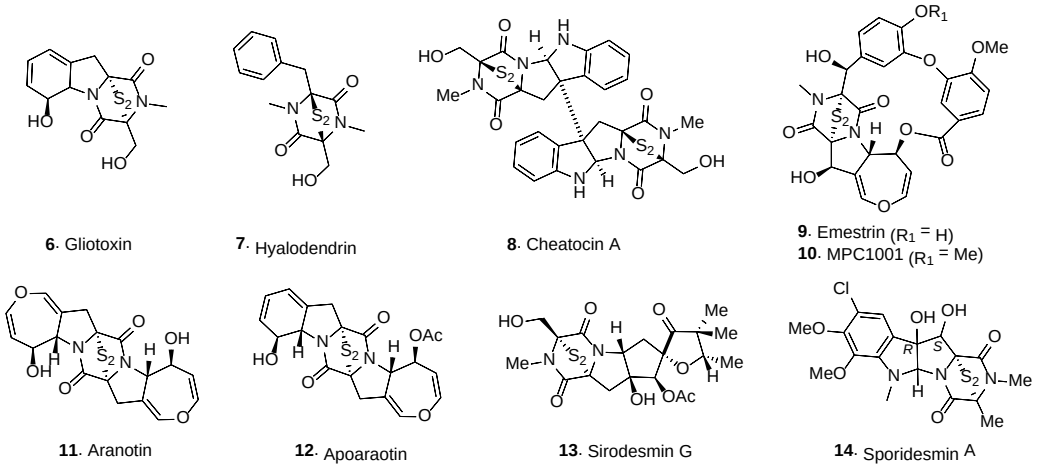


**Figure 2**. Examples of ETP containing natural products

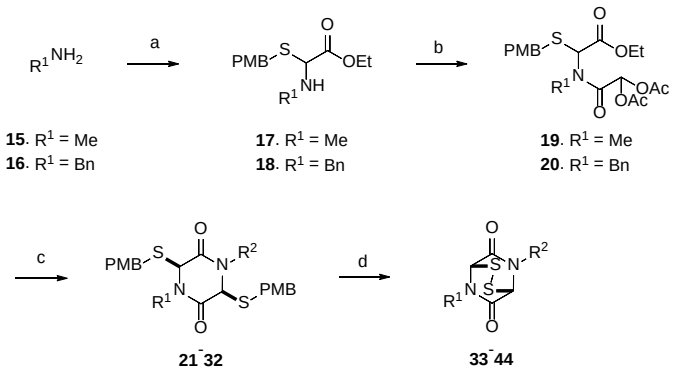

**15**. $R^1$ = Me
**16**. $R^1$ = Bn

**17**. $R^1$ = Me
**18**. $R^1$ = Bn

**19**. $R^1$ = Me
**20**. $R^1$ = Bn

**21**-**32**

**33**-**44**

**Scheme 1.** Synthesis route to dimeric ETP derivatives - reagents and conditions (a) ethyl glyoxalate, *p*-methoxybenzylmercaptan, toluene, 2 h, **17** - 37 %, **18** - 87 %; (b) 2-chloro-2-oxoethane-1,1-diyl diacetate, $NaHCO_3$, $CH_2Cl_2/H_2O$, 12 h, **19** - 97 %, **20** - 95 %; (c) *p*-methoxybenzylmercaptan, $R^2$-$NH_2$, DMAP, MeCN, 16 h, **21** - 62 %, **22** - 33 %, **23** - 65 %, **24** - 64 %, **25** - 54 %, **26** - 64 %, **27** - 68 %, **28** - 84 %, **29** - 61 %, **30** - 76 %, **31** - 70 %, **32** - 58 %; (d) 1. $BBr_3$, $CH_2Cl_2$, -78 °C 0.3 h, 2. $I_2$, RT, 0.5 h, **33**-**44** - 32-85 %.

Viral RNA was isolated from cell culture supernatants using the MagNA Pure LC System with the Total Nucleic Acid Isolation Kit (Roche Applied Science, Switzerland). Quantitative real-time reverse transcription polymerase chain reaction (RT-qPCR) was used to determine viral loads.[27] The remaining FL-4 cells were then subjected to a MTT cell viability assay to validate the RT-qPCR result, confirming it was not caused by non-specific toxicity and to provide a therapeutic index (Table 1). The toxicity and activity of azidothymidine (AZT) and Raltegravir were consistent with previous reports on FIV/HIV and were used as an internal standard and benchmark (**Table 1**).[28,29]

The limited toxicity observed in the initial screening with CrFK cells with 24-hours exposure may be a good indication that the compounds are not chronically toxic. However, there was increased toxicity with shorter chained substitutions (**33** & **35**-**37**). There was roughly an order of magnitude increase in toxicity when looking at the results for the longer-term FL-4 assay, which is consistent with previous results from this model.[25] The overall toxicity profile of the compounds (**33**-**44**) is encouraging as the ETP core is generally correlated to acute cytotoxicity. The results from prolonged exposure are particularly striking, as there was limited toxicity particularly for bulkier substitutions (**39**-**44**) and compounds that have functional groups that would assist with solubility, such as an ester (**41**-**43**). This likely enhancement in solubility is supported by the significantly lower melting points (<100 °C) of **41**-**43** compared to compound **33** (>200 °C).[30]

Poor solubility may have been a contributing factor to the weaker anti-viral efficacy of compound **33** and negligible therapeutic index. The addition of a benzyl group (**34**) did assist in increasing the potency 3-fold while not compromising the toxicity profile. Changing the methyl substituent to a *n*-butyl (**35**) also gave a slight boost in potency and an increase in cLogP, however the *iso*-propyl (**36**) and allyl (**37**) showed a decreased potency with respect to **35**. The di-substituted benzyl (**38**) showed the worst performance with the weakest potency of any analogue tested from this series and a 6-fold drop of compared with **35**, this could be in part due to an inability to cross the cell membrane. In stark contrast the 3-chloro substitution (**39**) showed an 8-fold increase in potency and a triple digit therapeutic index. The *p*-methoxybenzyl (**40**) demonstrated a slight increase in potency but a significant jump in toxicity brought the therapeutic index down to 57 from 184. However, the switch to an ester containing motif brought potency down to double digit nanomolar for compounds **41** and **42** with a therapeutic index above 300 for **42**. Compound **43** also performed well, but increased toxicity suppressed the therapeutic index. The naphthalene substitution (**44**) suffered the same fate as **38** with a decrease in potency and therapeutic index.

**Table 1.** Results of FIV and cytotoxicity screening on dimeric ETP derivatives

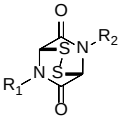

| Compound | Residue | | CrFK[a] | $CC_{50}$[b] | $EC_{50}$[b] | TI | clogP[c] |
|---|---|---|---|---|---|---|---|
| Number | $R_1$ | $R_2$ | % | µM | µM | | |
| **33** | Me | Me | 77 | >10 | 3 | >3 | 0.61 |
| **34** | benzyl | Me | >100 | >10 | 0.91 | >11 | 2.21 |
| **35** | benzyl | *n*-butyl | 63 | >10 | 0.63 | >16 | 3.8 |
| **36** | benzyl | *iso*-propyl | 50 | 6.5 | 1.6 | 4 | 3.05 |
| **37** | benzyl | allyl | 96 | 5.1 | 2.1 | 2.4 | 2.99 |
| **38** | benzyl | benzyl | >100 | 4.7 | 4 | 1.2 | 3.71 |
| **39** | benzyl | (3-chloro)benzyl | >100 | >100 | 0.55 | >184 | 4.43 |
| **40** | benzyl | (4-methoxy)benzyl | 99 | 5.4 | 0.41 | 57 | 3.63 |
| **41** | benzyl | ethyl 3-propanoate | >100 | >10 | 0.053 | >190 | 3.22 |
| **42** | benzyl | methyl 3-hexanoate | >100 | >10 | 0.034 | >300 | 3.29 |
| **43** | benzyl | ethyl 3-butanoate | >100 | 7.5 | 0.16 | 48 | 3.41 |
| **44** | benzyl | (methyl)napthalene | >100 | 7.2 | 1.9 | 4 | 4.89 |
| - | AZT | | >100 | >100 | 5.3 | 19 | -0.16 |
| - | Raltegravir | | >100 | >100 | 0.01 | >10000 | 1.16 |

[a]Sample concentration of compound in CrFK cells at 10 µM (% Viability); [b]Geometric mean, each concentration tested in triplicate after 7 days as a difference of the untreated cells; [c]Calculated using *Chemdraw Ultra 16*

In order to better understand the mechanics behind the possible mechanism of action we simulated the generalized ETP core to attempt to rationalize the results we observed (**Figure 3**). We visualized a combination of Jaguar minimized models showing HOMO orbital of one cysteine tooth (blue/red)[31] and single point fukui f- negative field (white/green) calculation for compound **42** and **34**. This demonstrated a propensity for a favorable reaction on the S-S of the ETP core structure (**Figure 3A-C**).

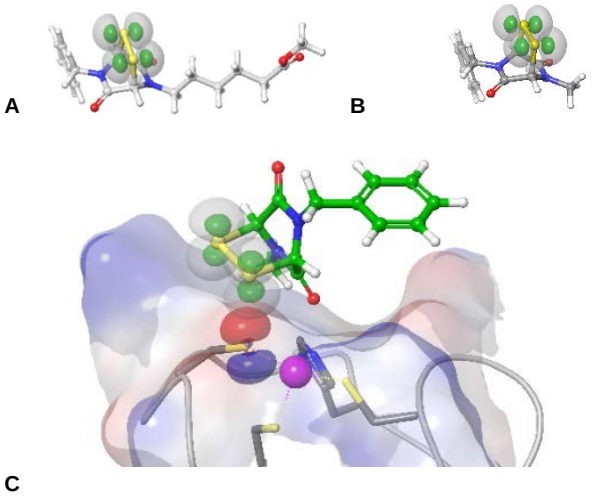


**Figure 3.** Visualization of negative components of condensed Fukui f-functions of with two isovalues 0.01 (white) and 0.002 (green). Minor Fukui f- surfaces are omitted for clarity: (a) negative Fukui F-functions of **42**; (b) negative fukui functions of **34**; (c) Simulation of **34** potential initial stage of the zinc ejection mechanism with the NCp CCHC zinc finger active site where Fukui f- functions are shown with two isovalues 0.01 (white) and 0.002 (green). In addition, HOMO-orbitals taken from Zinc finger model are shown.

We calculated the HOMO and LUMO orbitals of a simplified disubstituted epidithiodiketopiperazines ETP using density functional theory (DFT) and estimated the relative reactivity from atomic Fukui indices derived from frontier orbital theory (**Figure 4**).[32] Most reactivity of the core resided on the disulfide bridge, with substitutions appearing to only have a limited effect.

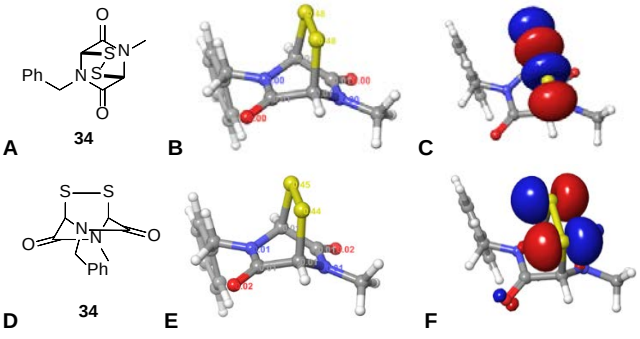


**Figure 4.** Investigation of reactive bond orbitals for cmpd **34** and general ETP cores (a) 2D representation of cmpd **34**; (b) HOMO orbital calculation for cmpd **34** (c) visual representation of HOMO orbital for cmpd **34**; (d) 3D representation of cmpd **34**; (e) LUMO orbital calculation for cmpd **34**; (f) visual representation of LUMO orbital for cmpd **34**.

The HOMO-LUMO gap for compound **34** is relatively small indicating why the compounds are stable in the ground state and not readily decomposing despite the ring strain (**Figure 4**). However, the ability of **34** to accept a nucleophilic attack appears more related to the puckered nature of the S-S bond (**Figure 4D**). The LUMO orbitals indicate that the S-S bond bridge can accept electrons, following to reorganisation effectively after bond dissociation. The S-S bond bridge is a key feature of the ETP core and sits above the rest of the structure.

We also wanted to investigate the conformation of the disubstituted ETP core and found the crystal structures of compounds **36**, **40**, **41** and **44** all crystallized in the monoclinic $P2_1/n$ space group (**Figure 5**).[33] The conformations of the ETP cores of all four molecules are virtually identical within the crystal structures and all bond lengths and angles do not deviate significantly from standard values in comparison with equivalent bond lengths and angles in the CSD.[34]

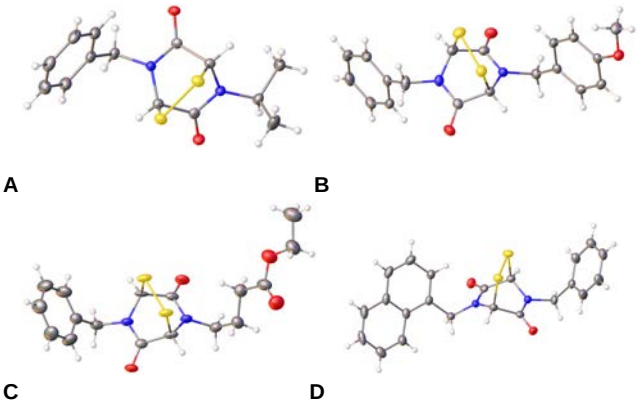


**Figure 5.** Crystal structure of compound **36**, **40, 41** & **44** showing bridged disulfide

During our investigation of the binding dynamics of the ETP structure we also observed through molecular docking using standard SP and qm-polarized docking, there was an overall poor convergence on target when orentating the structure to be set up for nucleophilic attack. This suggested that zinc abstraction, although driven mainly by disulfide bridge functionality does have an inital docking pose. The intial interaction begins with the coordination of carbonyl to zinc, where subsequently the sulfur atoms are close to solvent exposed cysteines. Watermap analysis utilising the Schrodinger suite confirmed placement of a water next to zinc supporting this hypothesis (**Figure 6A**).[35]

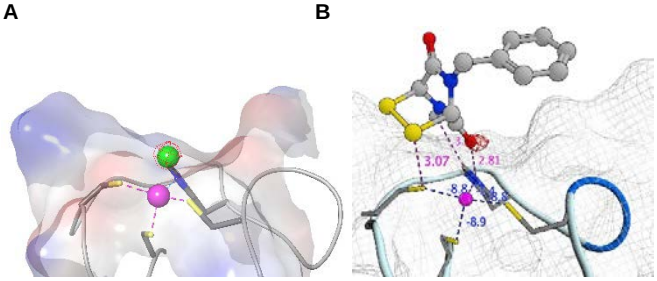


**Figure 6.** WaterMap analysis and docking (a) Confirmation of favourable water placement (-9.3 kcal/mol) (green ball showed placement of stable water molecule with red interaction field showing high free energy density. (b) grid type of MOE interaction potential for carbonyl oxygen of **34** (red grid field). MOE gives estimates of HB strengths shown with blue labels and selected distances in magenta.

This water can be usurped by the carbonyl of the ETP core structure. This observation is supported by interaction field analysis (MOE 2018.01, Chemical Computing Group) which placed the carbonyl in a favorable binding mode (**Figure 6B**).

We also investigated the conformation of the ETP core to examine the multi-substituted version of the ETP structure to see if perturbations near the carbonyl/disulphide would assist in increasing the overall anti-viral effect of the compounds. In order to achieve this, we designed and synthesized multi-substituent ETP analogs with small substituents next to the carbonyl and disulphide bridge (**Scheme 2**).

In order to access trisubstituted ETPs a similar approach when forming the di-substituted products (**33-44**) were used first forming ethyl 2-(allylamino)-2-((4-methoxybenzyl)thio)acetate (**46**) or **17** using allylamine (**45**) or **15** respectively under Dean and Stark conditions with ethyl glyoxalate and *p*-methoxybenzylmercaptan. The cyclisation diacetate precursor was formed by coupling 2-chloro-2-oxoethane-1,1-diyl diacetate to **46** and **17** to form **47** and **18**. These cyclisation intermediates (**47**) and **19** were treated with **15** or **45** to undergo a base catalysed cyclisation using DMAP and methanol to afford **48-51** in each of the corresponding substitution patterns. This enabled the access to a small tri-substituted array of analogs *via* treatment with lithium *bis*(trimethylsilyl)amide then an alkyl bromide in THF to afford (**52-56**). This step was achieved in good yields (49-78%), which enabled unmasking of the methoxy group with treatment of **52-56** with TFA and *p*-methoxybenzylmercaptan to afford the masked ETP precursors (**57-61**). These were treated with boron tribromide at -78°C to unmask the thiol before oxidation with iodine to afford the final tri-substituted ETP products (**62-65**) in good overall yields (21-28%).

To access the *tetra*-substituted allyl analog, **61** was treated with lithium *bis*(trimethylsilyl)amide then an alkyl bromide in THF to afford **66**. The precursor **66** was then unmasked with boron tribromide at -78°C and subsequently treated with iodine to afford the final ETP product in the array **67**.

Utilising the same screening cascade as before, we tested **6-8**, **62-65** and **67** for anti-viral efficacy and cytotoxicity (**Table 2**). The natural products **6-8** were particularly toxic. Compounds **6** and **7** were not screened in the anti-viral assay as **8** highlighted a connection between the acute toxicity and perceived anti-viral effect. Fortunately, we observed only limited toxicity with our multi-substituted ETP analogs **62-65** and **67**. Benchmarking these compounds to the disubstituted compounds **37** and **38**. Walking the allyl group around the dibenzyl ETP core significantly increased the anti-viral potency without increasing toxicity. Compound **62** demonstrated a 4-fold improvement in anti-viral efficacy with a significant improvement in the toxicity ratio with a therapeutic index about 80. **63** showed a 10-fold increase in potency, with a similar therapeutic index. **64** with the allyl now switched to the amino substitution showed an 8-fold increase toxicity with no improvement in anti-viral activity reducing the effective therapeutic window to below 10. **65** had poor aqueous solubility, likely accounting for lack of an activity profile. **67** has a similar anti-viral potency to **62**, highlighting the importance of the pendent benzyl substituents over the simple allyl.

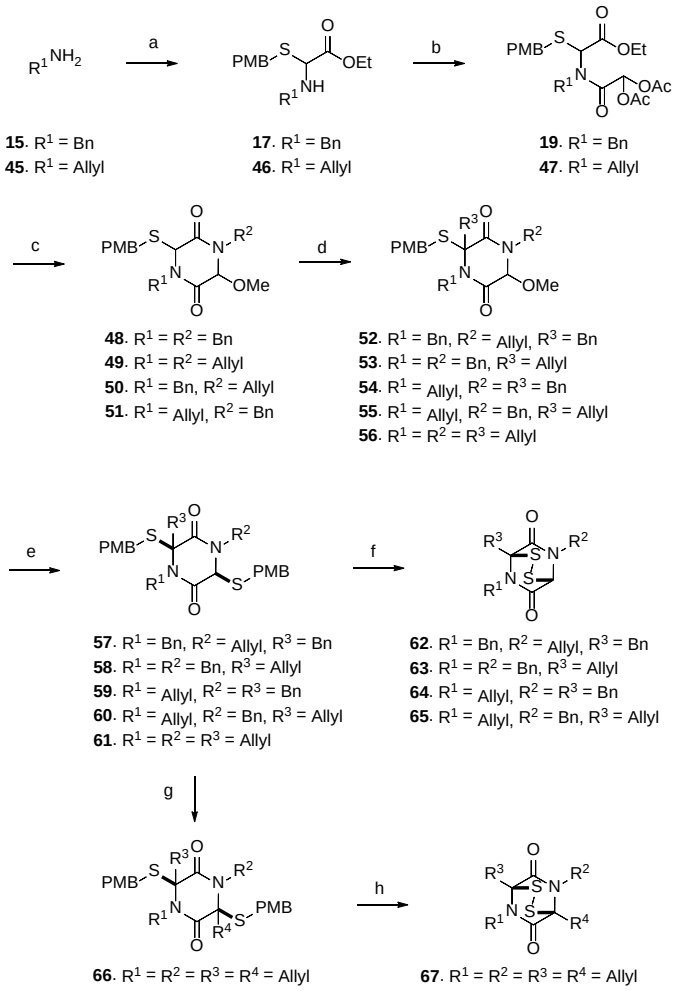


**Scheme 2.** Synthesis route to tri- and quad-meric ETP derivatives - reagents and conditions (a) ethyl glyoxalate, p-methoxybenzylmercaptan, toluene, 2h, **46** - 37%; (b) 2-chloro-2-oxoethane-1,1-diyl diacetate, $NaHCO_3$, $CH_2Cl_2/H_2O$, 12 h, **47** - 95 %; (c) $R^2$-$NH_2$, DMAP, MeOH, 5 h, **48** - 79%, **49** - 72%, **50** - 76% and **51** - 85%; (d) $R^3$-Br, LiHMDS, THF, 2.5 h, **52** - 49%, **53** - 79%, **54** - 78%, **55** - 68% and **56** - 65 %; (e) *p*-methoxybenzylmercaptan, TFA, $CH_2Cl_2$, 18 h, **57** - 81%, **58** - 83%, **59** - 82%, **60** - 78% and **61** - 63%; (f) 1. $BBr_3$, $CH_2Cl_2$, -78 °C 0.3 h, 2. $I_2$, RT, 0.5h, **62** - 23%, **63** - 24%, **64** - 21 % and **65** - 28%; (g) $R^4$-Br, LiHMDS, THF, 2.5h, **66** - 55%; (h) 1. $BBr_3$, $CH_2Cl_2$, -78 °C 0.3 h, 2. $I_2$, RT, 0.5 h, **67** - 41%.

The modelling of the Fukui indices of **63** (**Figure 7** and **8**), highlights the reactive potential of the ETP disulphide bridge. These values are consistent with previous reports,[25] and indicate that these compounds are available for nucleophilic attack and redox chemistry (**Figure 9**).

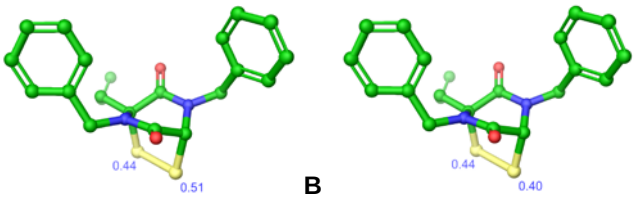


**Figure 7**. f_NN for **63** (a) LUMO indicates (b) HOMO indicates, highlighting the reactivity on the central ETP disulfide bridge.

**Table 2.** Results of FIV and cytotoxicity screening

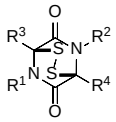

| Compound | Residue | | | | CrFK[a] | $CC_{50}$[b] | $EC_{50}$[b] | TI | clogP[c] |
|---|---|---|---|---|---|---|---|---|---|
| Number | $R^1$ | $R^2$ | $R^3$ | $R^4$ | % Viability | µM | µM | | |
| **6** | - | - | - | - | 6.1 | - | - | - | -0.03 |
| **8** | - | - | - | - | 11 | 0.0035 | 0.0017 | 2.1 | 1.21 |
| **7** | *N*-Me | *N*-Me | *N*-benzyl | *N*-methanol | 74 | - | - | - | 1.91 |
| **37** | *N*-benzyl | *N*-allyl | - | - | 96 | 5.1 | 2.1 | 2.4 | 2.99 |
| **38** | *N*-benzyl | *N*-benzyl | - | - | >100 | 4.7 | 3.9 | 1.2 | 3.71 |
| **62** | *N*-benzyl | *N*-allyl | *N*-benzyl | - | >100 | 79 | 0.89 | 88 | 4.92 |
| **63** | *N*-benzyl | *N*-benzyl | *N*-allyl | - | >100 | 6.0 | 0.088 | 69 | 4.92 |
| **64** | *N*-allyl | *N*-benzyl | *N*-benzyl | - | 85 | 0.72 | 0.11 | 6.7 | 4.92 |
| **65** | *N*-allyl | *N*-benzyl | *N*-allyl | - | >100 | >100 | >10 | - | 4.08 |
| **67** | *N*-allyl | *N*-allyl | *N*-allyl | *N*-allyl | 99 | 8.8 | 0.88 | 10 | 4.34 |

[a]Sample concentration of compound in CrFK cells at 10 µM (% Viability); [b]Geometric mean, each concentration tested in triplicate after 7 days as a difference of the untreated cells; [c]Calculated using *Chemdraw Ultra 16*

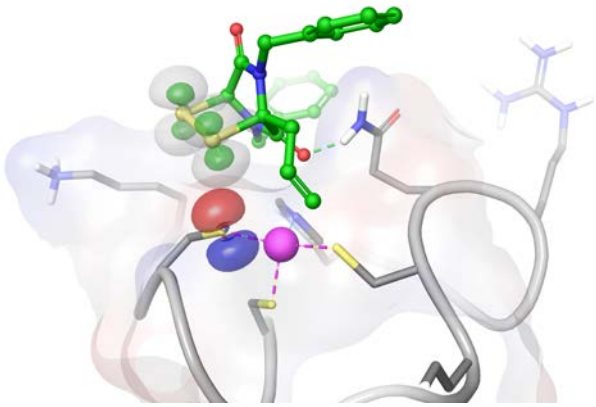

**Figure 8.** Visualization of negative values of Fukui f- functions with two isovalues 0.01 (green) and 0.003 (white) are shown. Simulation of **63** at the potential initial stage of the zinc ejection mechanism with the NCp CCHC zinc finger active site where Fukui f- functions are shown with two isovalues 0.01 (white) and 0.002 (green). In addition, HOMO-orbitals taken from Zinc finger model are shown.

Our proposed mechanism of action for the ETP core is consistent with previous reports, with the zinc-binding sites on the NCp of FIV which we determined using DFT calculations (**Figure 4**). The zinc ejection mechanism has previously been characterized with NMR and MS studies on HIV NCp7 and other targets, with an observable formation of protein-zinc-thiol(ate) complexes and several covalent modifications (**Figure 9**).[36,18a] We reasoned that ETP core mediated zinc ion ejection also occurs via an analogous FIV system in a similar mechanism to known zinc binding/disrupting compounds in which a zinc-binding cysteinyl thiol(ate) reacts with the disulfide of the core to generate a transient protein-ETP disulfide (**Figure 9**). This can rearrange to form an intramolecular protein disulfide with consequent reduction in zinc ion affinity. The ejected zinc ion (or zinc ETP core complex) could then complexes with a second (reduced) ETP core to form a stable complex which is analogous to work previously reported on the ETP class of natural products and some synthetic analogues.[18a]

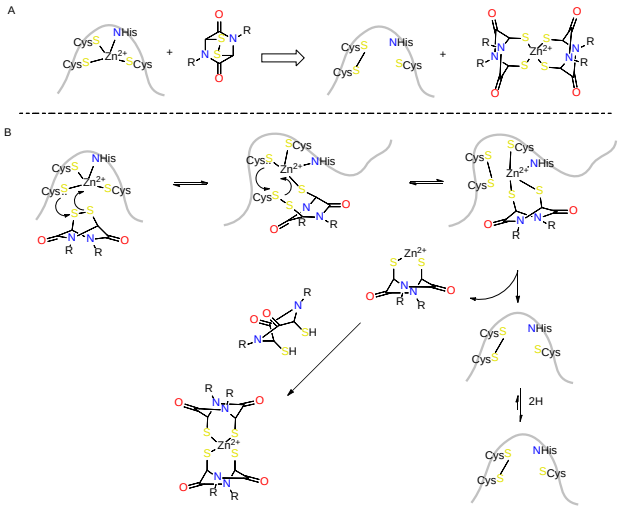

**Figure 9**. Proposed mechanism of action of the generalized ETP core for modification of NCp ***A*** - summary of the mechanism of zinc ejection from NCp/NCp7. ***B*** - a $Zn^{2+}$-coordinating cysteine thiol(ate) reacts with the disulfide of the ETP core to generate a transient intermediate disulfide. The disulfide then rearranges to form an intramolecular protein disulfide with consequent reduction in zinc ion affinity. The ejected zinc ion (or part $Zn^{2+}$ complex) can then complex with a second ETP core (reduced) to form a stable complex.

To further support the observed activity and proposed mechanism of action we sought to show that disrupted disulfides were less active. The focus of this work builds on the idea that the disulphide bridge is pivotal to the activity of the compounds against the NCp target. We synthesized two disrupted disulfides on a simple dibenzyl scaffold (**Scheme 3**). The first was produced from glycine anhydride (**68**) over 4 steps to produce the dithiol version of the dibenzyl ETP (**69**) from literature precedent.[18a] The second derivative was made by reducing the disulphide bridge of **38** with sodium borohydride and then treating with pyridine and iodomethane in methanol to afford the dimethyl derivative (**70**).

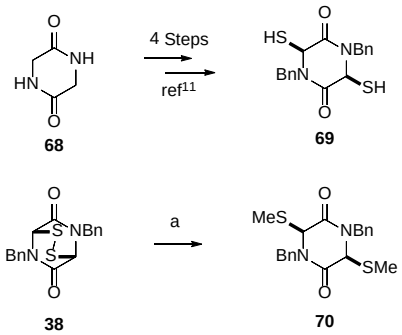


**Scheme 3**. Synthesis route to access dithiol derivative (**69**) and dimethyl derivative (**70**). Reagents and conditions: a) i) $NaBH_4$ ii) pyridine, MeOH, MeI, 3h, 80 % over two steps.

These two control compounds support our proposed mechanism of action with a limited amount of activity observed in the dithiol derivative (**69**) and no activity in the totally blocked dimethyl derivative (**70**) (**Table 3**).

**Table 3.** Results of FIV and cytotoxicity screening of **65** and **70**

| Compound | CrFK[a] | $CC_{50}$[b] | $EC_{50}$[b] |
|---|---|---|---|
| Number | Viability | μM | μM |
| **69** | >100 | 15 | 1.8 |
| **70** | 96 | >100 | >100 |

[a]Sample concentration of compound in CrFK cells at 10 μM (% Viability); [b]Geometric mean, each concentration tested in triplicate after 7 days as a difference of the untreated cells.

## Conclusions

The nanomolar potencies of these compounds coupled with light toxicities are a significant step forward in the design and utilization of the ETP scaffold as a functional series beyond generic toxicity. This is only the second report of reduced toxicity with the ETP core by structural simplification.[37] This investigation of the ETP core serves to highlight the potential of the ETP core for versatile applications beyond cancer. It is also an indication that the zinc abstraction mechanism and/or the ETP core does not automatically equate to a toxic pharmacophore. The therapeutic index of the ester containing compounds (**41**-**43**) and **63**-**64** were particularly encouraging and highlighting the need for more investigation of this privileged core. These focused libraries demonstrate there is scope for potential optimization beyond the narrow structure activity relationships we have observed, with a possibility for progression towards a candidate compound for targeting the FIV/HIV nucleocapsid protein. The ETP core and functionality while relatively under-explored still have the potential to generate a pre-clinical candidate to treat both FIV and HIV in an *in-vivo* setting.

## Chemistry

### General chemistry section

All reactions requiring the use of dry conditions were carried out under an atmosphere of nitrogen and all glassware was pre-dried in an oven (110 °C) and cooled under nitrogen prior to use. Stirring was by internal magnetic follower unless otherwise stated. Microwave heated reactions were carried out in a Biotage™ Initiator 2.5. All reactions were followed by TLC and organic phases extracted were dried with anhydrous magnesium sulfate or sodium sulfate as required. TLC analysis was carried out using Merck aluminium-backed plates coated with silica gel 60 $F_{254}$. Components were visualised using combinations of ultraviolet light, iodine and ceric ammonium molybdate stain. All anhydrous solvents and reagents were purchased from Sigma-Aldrich and Fisher Scientific and used with Oxford sure/seal valves attached to a standard Schlenk line for solvent removal.

Purification of compounds was carried out using two different methodologies: flash column chromatography (FCC) as reported by Still *et al* or by automatic column chromatography (ACC).[38] Silica gel used for FCC was Merck 60 (230-400 mesh). ACC was carried out using a Biotage™ Horizon High Performance Flash Chromatography (HPFC). The use of this automated system required different pre-packed silica columns supported by the system and supplied by Biotage™. Columns used were: Flash 12+S, Flash 12+M, Flash 25+S, Flash 25+M, SNAP 10 g, SNAP 25 g, SNAP 50 g, SNAP 100 g, ZIP 5 g, ZIP 10 g, ZIP 30 g and ZIP 45 g cartridges.

Infrared spectra were recorded on a Bruker Alpha FT-IR spectrophotometer using NaCl plates. $^1$H NMR and $^{13}$C NMR were recorded using either a Bruker AM400 spectrometer operating at 400 MHz for proton and 101 MHz for carbon or a Bruker AM500 spectrometer operating at 500 MHz for proton and 126 MHz for carbon. Chemical shifts ($\delta_H$ and $\delta_C$) are quoted as parts per million downfield from 0. The multiplicity of a $^1$H NMR signal is designated by one of the following abbreviations: s = singlet, d = doublet, t = triplet, q = quartet, br = broad and m = multiplet. Coupling constants (J) are expressed in Hertz. High-resolution mass spectra were carried out using either a Kratos MS89MS with Kratos DS90 software or a Jeol AX505W with Jeol complement data system. Samples were ionised electronically (EI), with an accelerating voltage of ≈6kV or by low-resolution fast atom bombardment (FAB) in a thioglycerol matrix. High-resolution fast atom bombardment was carried out at the ULIRS mass spectrometry facility at UCL School of Pharmacy.

### General method formation of 17, 18 and 46

Amine (25.2 mmol) was added to a solution of ethyl glyoxalate (5.0 mL of a 50% solution in toluene, 25.2 mmol) in toluene (20.0 mL) at room temperature (RT) and stirred for 2 minutes, whereupon *para*-methoxybenzyl mercaptan (25.2 mmol) was added and the mixture stirred for 2 hours. Solvent was removed under reduced pressure and the residue purified *via* Biotage™ Horizon to give the desired amide (**17**, **18** and **46**).

### General method formation of 19, 20 and 47

A solution of 2-chloro-2-oxoethane-1,1-diyl diacetate (26.3 mmol) in dichloromethane (20.0 mL) was added dropwise to a rapidly stirred biphasic mixture of previously synthesised amide (21.9 mmol) and sodium hydrogen carbonate (153 mmol) in dichloromethane (150 mL) and water (100 mL) at RT and the resulting mixture stirred rapidly for 12 hours. The layers were separated and the aqueous phase extracted with dichloromethane (2 x 100 mL). The combined extracts were dried over $MgSO_4$, filtered and solvent removed under reduced pressure to give desired diacetate amide intermediate that did not require further purification (**19**, **20** and **47**).

**General method formation of 21-32**

Amine (1.58 mmol) was added to a solution of the diacetate amide intermediate (0.53 mmol) in acetonitrile (15.0 mL) followed by addition *para*-methoxybenzyl mercaptan (0.79 mmol) and the resulting mixture stirred for 2 minutes. DMAP (0.26 mmol) was added and the resulting mixture heated at reflux for 16 hours, cooled to RT and solvent removed under reduced pressure. The residue was purified *via* Biotage™ Horizon and, when possible, recrystallised to give the desired diketopiperazine (**21**-**32**).

**General method formation of 33-44, 62-65 and 67**

Boron tribromide (0.56 mmol) was added dropwise to a solution of the diketopiperazine (0.28 mmol) in dichloromethane (10.0 mL) at -78 °C. The resulting mixture was stirred for 30 minutes whereupon sodium hydrogen carbonate (10.0 mL of a saturated aqueous solution) was added and the biphasic mixture stirred for 15 minutes until the yellow colour had dissipated. The resulting mixture was stirred at room temperature for 40 minutes, whereupon iodine was added portionwise until the colour due to iodine just persisted and stirring was maintained for 5 minutes. A solution of saturated aqueous sodium thiosulfate was added and the mixture stirred for 30 minutes, diluted with dichloromethane (10.0 mL) and water (20.0 mL). The layers were separated and the aqueous phase extracted with dichloromethane (2 x 20.0 mL). The combined organic extracts were dried over $MgSO_4$, filtered and solvent removed under reduced pressure. The residue was purified *via* Biotage™ Horizon and, when possible, recrystallized (ethyl acetate/hexane) to give the desired epidithiodiketopiperazines (**33**-**44**, **62**-**65** and **67**).

**Characterization of 30-44**

**(±)-(1S,4S)-2,5-Dimethyl-7-thia-2,5-diazabicyclo[2.2.1]heptane-3,6-dione 7-sulfide (33)** Pale yellow solid (70 mg, 68%); m.p. 202-205 °C; IR: $\nu_{max}$/cm$^{-1}$ 1686 (C=O), 1390 ($CH_3$); δ H (400 MHz; $CDCl_3$) 3.05 (6H, s, NC$H_3$), 5.15 (2H, s, C*H*S); δ C (101 MHz, $CDCl_3$) 31.59 (N**C**H$_3$), 67.60 (**C**HS), 164.32 (**C**O); *m/z* 202 (100%, [M-H]$^-$): Found [M-H]$^-$ 202.9957, $C_6H_7N_2O_2S_2$ requires 202.9949. Consistent with previous report.[39]

**(±)-(1S,4S)-2-Benzyl-5-methyl-7-thia-2,5-diazabicyclo[2.2.1]heptane-3,6-dione 7-sulfide (34)** Pale yellow solid (70 mg, 65%); m.p. 109-111 °C; IR: $\nu_{max}$/cm$^{-1}$ 1699 (C=O); δ H (400 MHz; $CDCl_3$) 3.12 (3H, s, NC$H_3$), 4.49 (1H, d, *J* 12.9, NC$H_2$), 4.90 (1H, d, *J* 12.9, NC$H_2$), 5.20 (1H, s, C*H*S), 5.32 (1H, s, C*H*S), 7.28 – 7.39 (5H, m, Ar-*H*); δ C (101 MHz, $CDCl_3$) 31.4 (N**C**H$_3$), 47.5 (**C**H$_2$), 64.3 (**C**HS), 67.5 (**C**HS), 128.4 (Ar-**C**-H), 128.6 (Ar-**C**-H), 129.2 (Ar-**C**-H), 134.0 (quaternary **C**), 163.9 (**C**O), 164.0 (**C**O); *m/z* 281 (100%, [M+H]$^+$): Found [M+H]$^+$ 281.0415, $C_{12}H_{13}N_2O_2S_2$ requires 281.0418. Consistent with previous report.[23a]

**(±)-(1S,4S)-2-Benzyl-5-butyl-7-thia-2,5-diazabicyclo[2.2.1]heptane-3,6-dione 7-sulfide (35)** Pale yellow solid (80 mg, 54%); m.p. 119-121 °C; IR: $\nu_{max}$/cm$^{-1}$ 1681 (C=O); δ H (400 MHz; $CDCl_3$) 0.95 (3H, t, *J* 7.3, $NCH_2(CH_2)_2CH_3$), 1.29 – 1.37 (2H, m, $NCH_2(CH_2)_2CH_3$), 1.61 – 1.72 (2H, m, $NCH_2(CH_2)_2CH_3$), 3.42 – 3.59 (2H, m, $NCH_2(CH_2)_2CH_3$), 4.51 (1H, d, *J* 14.9, NC$H_2$-Ph), 4.84 (1H, d, *J* 14.9, NC$H_2$-Ph), 5.18 (1H, s, C*H*S), 5.34 (1H, s, C*H*S), 7.26 – 7.29 (2H, m, Ar-*H*), 7.31 – 7.38 (3H, m, Ar-*H*); δ C (101 MHz; $CDCl_3$) 13.7 (**C**H$_3$), 19.9 (**C**H$_2$), 29.8 (**C**H$_2$), 44.9 (**C**H$_2$), 47.7 (**C**H$_2$), 64.7 (**C**HS), 65.6 (**C**HS), 128.4 (Ar-**C**-H), 128.6 (Ar-**C**-H), 129.1 (Ar-**C**-H), 134.1 (quaternary **C**), 163.5 (**C**O), 164.0 (**C**O); *m/z* 323 (100%, [M+H]$^+$): Found [M+H]$^+$ 323.0900, $C_{15}H_{19}N_2O_2S_2$ requires 323.0888. Consistent with previous report.[23a]

**(±)-(1S,4S)-2-Benzyl-5-isopropyl-7-thia-2,5-diazabicyclo[2.2.1]heptane-3,6-dione 7-sulfide (36)** Pale yellow solid (40 mg, 65%); m.p. 177-180 °C; IR: $\nu_{max}$/cm$^{-1}$ 1662 (C=O), 1609 (C=C), 1434 (C-H), 731 (C-H); δ H (400 MHz; $CDCl_3$) 1.35 (6H, dd, *J* 12.9 & 6.8, $CH(CH_3)_2$), 1.61 (1H, s, $CH(CH_3)_2$), 4.53 (1H, d, *J* 12.6, NC$H_2$-Ph), 4.83 (1H, d, *J* 12.9, NC$H_2$-Ph), 5.19 (1H, s, C*H*S), 5.48 (1H, s, C*H*S), 7.30 (3H, d, *J* 10.0, Ar-*H*), 7.39 (2H, d, *J* 7.4, Ar-*H*); δ C (101 MHz, $CDCl_3$) 19.8 (**C**H$_3$), 20.7 (**C**H$_3$), 46.6 (**C**H), 48.0 (**C**H$_2$), 61.0 (**C**HS), 65.3 (**C**HS), 128.6 (Ar-**C**-H), 128.8 (Ar-**C**-H), 129.3 (Ar-**C**-H), 134.4 (quaternary **C**), 163.0 (**C**O), 164.3 (**C**O); *m/z* 331 (100%, [M+Na]$^+$): Found [M+Na]$^+$ 331.0569, $C_{14}H_{16}N_2O_2S_2Na$ requires 331.0551. Consistent with previous report.[23a]

**(±)-(1S,4S)-2-Allyl-5-benzyl-7-thia-2,5-diazabicyclo[2.2.1]heptane-3,6-dione 7-sulfide (37)** Pale yellow solid (30 mg, 60%); m.p. 116-118 °C; IR: $\nu_{max}$/cm$^{-1}$ 1685 (C=O); δ H (400 MHz; $CDCl_3$) 3.96 (1H, dd, *J* 15.4 & 8.6, NC$H_2$CH=CH$_2$), 4.25 (1H, dd, *J* 15.4 & 7.6, NC$H_2$CH=CH$_2$), 4.49 (1H, d, *J* 11.7, NC$H_2$), 4.85 (1H, d, *J* 11.9, NC$H_2$), 5.22 (1H, s, C*H*S), 5.33 – 5.34 (2H, m, CH=C$H_2$), 5.36 (1H, s, C*H*S), 5.38 – 5.42 (1H, m, C*H*=CH$_2$), 7.26 – 7.29 (2H, m, Ar-*H*), 7.32 – 7.39 (3H, m, Ar-*H*); δ C (101 MHz, $CDCl_3$) 46.4 (**C**H$_2$), 47.5 (**C**H$_2$), 64.4 (**C**HS), 64.6 (**C**HS), 120.7 (CH**C**H$_2$), 128.3 (Ar-**C**-H), 128.5 (Ar-**C**-H), 129.1 (Ar-**C**-H), 130.7 (**C**H=CH$_2$), 134.1 (quaternary **C**), 163.4 (**C**O), 163.8 (**C**O); *m/z* 307 (100%, [M+H]$^+$): Found [M+H]$^+$ 307.0484, $C_{14}H_{15}N_2O_2S_2$ requires 307.0497. Consistent with previous report.[18a]

**(±)-(1S,4S)-2,5-Dibenzyl-7-thia-2,5-diazabicyclo[2.2.1]heptane-3,6-dione 7-sulfide (38)** Pale yellow solid (100 mg, 85%); m.p. 166-188 °C; IR: $\nu_{max}$/cm$^{-1}$ 1685 (C=O); δ H (400 MHz; $CDCl_3$) 4.63 (2H, d, *J* 12.0, C$H_2$Ar), 4.99 (2H, d, *J* 12.0 Hz, C$H_2$Ar), 5.39 (2H, s, C*H*S), 7.40 – 7.54 (10H, m, Ar-*H*); δ C (101 MHz, $CDCl_3$) 48.1 (**C**H$_2$), 65.1 (**C**H), 128.85 (Ar-**C**-H), 129.0 (Ar-**C**-H), 129.6 (Ar-**C**-H), 134.5 (quaternary **C**), 164.2 (**C**O); *m/z* 357 (100%, [M+H]$^+$): Found [M+H]$^+$ 357.0651, $C_{18}H_{17}N_2O_2S_2$ requires 357.0653. Consistent with previous report.[23a]

**(±)-(1S,4S)-2-Benzyl-5-(3-chlorobenzyl)-7-thia-2,5-diazabicyclo [2.2.1]heptane-3,6-dione 7-sulfide (39)** Pale yellow solid (140 mg, 32%); m.p. 147-149 °C; IR: $\nu_{max}$/cm$^{-1}$ 1674 (C=O); δ H (400 MHz; $CDCl_3$) 4.50 – 4.52 (2H, m, NC$H_2$Ar), 4.72 (1H, d, *J* 11.1, NC$H_2$), 4.84 (1H, d, *J* 11.9, NC$H_2$), 5.26 (1H, s, C*H*S), 5.27 (1H, s, C*H*S), 7.18 – 7.19 (1H, m, Ar-*H*), 7.26 – 7.40 (8H, m, Ar-*H*); δ C (101 MHz, $CDCl_3$) 47.2 (N**C**H$_2$), 47.7 (N**C**H$_2$), 64.5 (**C**HS), 64.9 (**C**HS), 126.3 (Ar-**C**-H), 128.4 (Ar-**C**-H), 128.4 (Ar-**C**-H), 128.6 (Ar-**C**-H), 128.7 (Ar-**C**-H), 129.1 (Ar-**C**-H), 130.4 (Ar-**C**-H), 134.0 (quaternary **C**), 134.9 (quaternary **C**), 136.3 (quaternary **C**), 163.6 (**C**O), 163.7 (**C**O); *m/z* 391.0853 (100%, [M+H]$^+$), 392.0931 (27.6%, [M+H]$^+$), 393.0873 (42.3%, [M+H]$^+$), 394.0934 (14.1%, [M+H]$^+$), 395.0991 (13.9%, [M+H]$^+$), $C_{18}H_{16}ClN_2O_2S_2$ requires 391.0842. Consistent with previous report.[23a]

**(±)-(1S,4S)-2-Benzyl-5-(4-methoxybenzyl)-7-thia-2,5-diazabicyclo[2.2.1] heptane-3,6-dione 7-sulfide (40)** Pale yellow solid (110 mg, 48%); m.p. 146-148 °C; IR: $\nu_{max}/cm^{-1}$ 2991 (C-H), 1681 (C=O); δ H (400 MHz; $CDCl_3$) 3.80 (3H, s, OC*H*$_3$), 4.43 (1H, d, *J* 12.7, C*H*$_2$), 4.48 (1H, d, *J* 13.0, C*H*$_2$), 4.75 (1H, d, *J* 12.7, C*H*$_2$), 4.82 (1H, d, *J* 13.0, C*H*$_2$), 5.25 (1H, s, C*H*S), 5.26 (1H, s, C*H*S), 6.90 (2H, d, *J* 8.6, Ar-*H*), 7.21 (2H, d, *J* 8.6, Ar-*H*), 7.27 – 7.29 (2H, m, Ar-*H*), 7.35 – 7.36 (3H, m, Ar-*H*); δ C (101 MHz, $CDCl_3$) 47.1 (**C**H$_2$), 47.6 (**C**H$_2$), 55.2 (O**C**H$_3$), 64.3 (**C**HS), 64.7 (**C**HS), 114.5 (Ar-**C**-H), 100.8 (quaternary **C**), 128.3 (Ar-**C**-H), 128.5 (Ar-**C**-H), 129.1 (Ar-**C**-H), 129.9 (Ar-**C**-H), 134.1 (quaternary **C**), 159.7 (quaternary **C**), 163.6 (**C**O), 163.8 (**C**O); *m/z* 387 (100%, $[M+H]^+$): Found $[M+H]^+$ 387.0833, $C_{19}H_{19}N_2O_3S_2$ requires 387.0837. Consistent with previous report.[23a]

**Ethyl 3-((±)-(1S,4S)-5-benzyl-3,6-dioxo-7-sulfido-7-thia-2,5-diazabicyclo [2.2.1]heptan-2-yl)propanoate (41)** Pale yellow solid (50 mg, 51%); m.p. 100-104 °C; $\nu_{max}/cm^{-1}$ 1670 (C=O), 1496 (C-H); δ H (400 MHz; $CDCl_3$) 1.30 (3H, t, *J* 7.1, OCH$_2$C*H*$_3$), 2.71 (2H, t, *J* 6.2, NC*H*$_2$), 3.79 – 3.84 (2H, m, NCH$_2$C*H*$_2$), 4.22 (2H, q, *J* 7.1, OC*H*$_2$CH$_3$), 4.50 (1H, d, *J* 15.0, NC*H*$_2$), 4.86 (1H, d, *J* 15.0, NC*H*$_2$), 5.19 (1H, s, C*H*S), 5.67 (1H, s, C*H*S), 7.28 – 7.29 (1H, m, Ar-*H*), 7.30 (1H, d, *J* 2.0, Ar-*H*), 7.38 (2H, t, *J* 2.1, Ar-*H*), 7.39 – 7.40 (1H, m, Ar-*H*); δ C (101 MHz; $CDCl_3$) 14.4 (**C**H$_3$), 33.0 (**C**H$_2$), 41.9 (**C**H$_2$), 47.9 (**C**H$_2$), 61.5 (**C**H$_2$), 64.8 (**C**HS), 67.0 (**C**HS), 128.6 (Ar-**C**-H), 128.8 (Ar-**C**-H), 129.4 (Ar-**C**-H), 134.5 (quaternary **C**), 163.6 (**C**O), 164.1 (**C**O), 171.7 (**C**O); *m/z* 389 (100%, $[M+Na]^+$): Found $[M+Na]^+$ 389.0622, $C_{16}H_{18}N_2O_4S_2Na$ requires 389.0606. Consistent with previous report.[23a]

**Methyl 6-((±)-(1S,4S)-5-benzyl-3,6-dioxo-7-sulfido-7-thia-2,5-diazabicyclo[2.2.1]heptan-2-yl)hexanoate (42)** Pale yellow solid; (70 mg, 75%); m.p. 85-88 °C; IR: $\nu_{max}/cm^{-1}$ 2933 (C-H), 1734 (C=O), 1674 (C=O), 1451 (CH$_2$), 733 (C-H); δ H (400 MHz; $CDCl_3$) 1.36 – 1.42 (2H, m, NCH$_2$(C*H*$_2$)$_3$CH$_2$CO), 2.34 (2H, t, *J* 7.4, NCH$_2$(C*H*$_2$)$_3$CH$_2$CO), 3.53 (2H, t, *J* 7.3, NCH$_2$(C*H*$_2$)$_3$CH$_2$CO), 3.68 – 3.69 (5H, m, C*H*$_2$CO$_2$C*H*$_3$), 3.73 – 3.80 (2H, m, NC*H*$_2$(CH$_2$)$_3$CH$_2$CO), 4.52 (1H, d, *J* 12.0, NC*H*$_2$-Ph), 4.85 (1H, d, *J* 12.0, NC*H*$_2$-Ph), 5.20 (1H, s, C*H*S), 5.37 (1H, s, C*H*S), 7.30 (2H, d, *J* 7.7, Ar-*H*), 7.37 – 7.40 (3H, m, Ar-*H*); δ C (101 MHz, $CDCl_3$) 24.6 (**C**H$_2$), 26.3 (**C**H$_2$), 27.6 (**C**H$_2$), 34.0 (**C**H$_2$), 45.3 (**C**H$_2$), 47.9 (**C**H$_2$), 51.7 (**C**H$_3$), 64.9 (**C**HS), 65.8 (**C**HS), 128.6 (Ar-**C**-H), 128.8 (Ar-**C**-H), 129.3 (Ar-**C**-H), 134.3 (quaternary **C**), 163.8 (**C**O), 164.2 (**C**O), 174.0 (**C**O); *m/z* 417 (100%, $[M+Na]^+$): Found $[M+Na]^+$ 417.0939, $C_{18}H_{22}N_2O_4S_2Na$ requires 417.0919. Consistent with previous report.[23a]

**Ethyl 4-((±)-(1S,4S)-5-benzyl-3,6-dioxo-7-sulfido-7-thia-2,5-diazabicyclo [2.2.1]heptan-2-yl)butanoate (43)** Pale yellow solid (50 mg, 64%); m.p. 82-84 °C; IR: $\nu_{max}/cm^{-1}$ 1498 (CH$_2$), 1160 (C-C(O)-C); δ H (400 MHz; $CDCl_3$) 1.28 (3H, t, *J* 7.1, OCH$_2$C*H*$_3$), 1.99 – 2.09 (2H, m, NCH$_2$C*H*$_2$CH$_2$CO), 2.40 – 2.43 (2H, m, NC*H*$_2$CH$_2$CH$_2$CO), 3.52 – 3.67 (2H, m, NCH$_2$CH$_2$C*H*$_2$CO), 4.17 – 4.20 (2H, m, OC*H*$_2$CH$_3$), 4.53 (1H, d, *J* 12.0, NC*H*$_2$-Ph), 4.86 (1H, d, *J* 12.2, NC*H*$_2$-Ph), 5.20 (1H, s, C*H*S), 5.42 (1H, s, C*H*S), 7.29 – 7.32 (2H, m, Ar-*H*), 7.36 – 7.41 (3 H, m, Ar-*H*); δ C (101 MHz, $CDCl_3$) 14.4 (**C**H$_3$), 23.3 (**C**H$_2$), 31.2 (**C**H$_2$), 44.9 (**C**H$_2$), 48.0 (**C**H$_2$), 60.9 (**C**H$_2$), 64.9 (**C**HS), 66.1 (**C**HS), 128.7 (Ar-**C**-H), 128.8 (Ar-**C**-H), 129.4 (Ar-**C**-H), 134.3 (quaternary **C**), 163.9 (**C**O), 164.1 (**C**O), 172.7 (**C**O); *m/z* 403 (100%, $[M+Na]^+$): Found $[M+Na]^+$ 403.1341, $C_{17}H_{20}N_2O_4S_2Na$ requires 403.0762. Consistent with previous report.[23a]

**(±)-(1S,4S)-2-Benzyl-5-(naphthalen-1-ylmethyl)-7-thia-2,5-diazabicyclo [2.2.1]heptane-3,6-dione 7-sulfide (44)** Pale yellow solid (180 mg, 85%); m.p. 161-163 °C; IR: $\nu_{max}/cm^{-1}$ 1685 (C=O); δ H (400 MHz; $CDCl_3$) 4.40 (1H, d, *J* 12.6, NC*H*$_2$), 4.79 – 4.84 (3H, m, NC*H*$_2$), 5.24 (1H, s, C*H*S), 5.30 (1H, s, C*H*S), 7.20 – 7.25 (2H, m, Ar-*H*), 7.34 – 7.39 (3H, m, Ar-*H*), 7.44 – 7.47 (2H, m, Ar-*H*), 7.53 – 7.58 (2H, m, Ar-*H*), 7.88 – 7.92 (2H, m, Ar-*H*), 7.95 – 8.00 (1H, m, Ar-*H*); δ C (101 MHz, $CDCl_3$) 45.1 (**C**H$_2$), 47.3 (**C**H$_2$), 63.4 (**C**HS), 64.6 (**C**HS), 123.1 (Ar-**C**-H), 100.1 (Ar-**C**-H), 126.3 (Ar-**C**-H), 126.9 (Ar-**C**-H), 128.1 (Ar-**C**-H), 128.4 (Ar-**C**-H), 128.4 (Ar-**C**-H), 128.8 (Ar-**C**-H), 129.0 (Ar-**C**-H), 129.5 (quaternary **C**), 129.9 (Ar-**C**-H), 131.5 (quaternary **C**), 133.8 (quaternary **C**), 134.1 (quaternary **C**), 163.4 (**C**O), 163.5 (**C**O); *m/z* 407 (100%, $[M+H]^+$): Found $[M+H]^+$ 407.0791, $C_{22}H_{19}N_2O_2S_2$ requires 407.0810. Consistent with previous report.[23a]

**General Method formation of 48-51**

Amine (1.93 mmol) was added to a solution of previously synthesised diacetate amide intermediate (1.29 mmol) in methanol (15.0 mL) and the resulting mixture stirred for 2 minutes. DMAP (0.64 mmol) was added and the resulting mixture was stirred for 5 hours at RT and solvent removed under reduced pressure. The residue was purified *via* Biotage™ Horizon and recrystallised to give the desired methoxy intermediate (**48-51**).

**General Method formation of 52-56**

LiHMDS (1M solution in tetrahydrofuran, 0.34 mmol) was added dropwise to a solution of the previously synthesised methoxy intermediate (0.17 mmol) and halogenoalkane (0.84 mmol) in tetrahydrofuran (2.00 mL) at -78 °C and the resulting mixture was stirred at this temperature for 1 hour and 1.5 hours at 0 °C. Saturated aqueous sodium hydrogen carbonate (10.0 mL) was added and solvent removed under reduced pressure. The residue was partitioned between water (10.0 mL) and dichloromethane (20.0 mL). The aqueous phase was extracted with dichloromethane (2 x 10.0 mL) and the combined extracts were dried ($MgSO_4$), filtered and solvent removed under reduced pressure. The residue was purified *via* Biotage™ Horizon to give the desired tri-substituted methoxy intermediate (**52-56**).

**General Method formation of 57-61**

TFA (9.17 mmol) was added to a solution of tri-substituted methoxy intermediate (0.61 mmol) in dichloromethane (10.0 mL) at RT followed by the addition of *para*-methoxybenzyl mercaptan (0.92 mmol) and the resulting mixture was stirred at this temperature for 18 hours. After, the solution was diluted in dichloromethane (10.0 mL) and washed with saturated aqueous sodium hydrogen carbonate (10.0 mL). The aqueous phase was extracted with dichloromethane (2 x 10.0 mL) and the combined extracts were dried ($MgSO_4$), filtered and solvent removed under reduced pressure. The residue was purified *via* Biotage™ Horizon and recrystallised (ethyl acetate/hexane) to give the desired diketopiperazine (**57-61**).

**Method formation of 66**

LiHMDS (1M solution in tetrahydrofuran, 0.68 mmol) was added dropwise to a solution of **61** (0.17 mmol) and allyl bromide (1.68 mmol) in tetrahydrofuran (2.0 mL) at -78 °C and the resulting mixture was stirred at this temperature for 1 hour and 1.5 hours at

0 °C. Saturated aqueous sodium hydrogen carbonate (10.0 mL) was added and solvent removed under reduced pressure. The residue was partitioned between water (10.0 mL) and dichloromethane (20.0 mL). The aqueous phase was extracted with dichloromethane (2 x 10.0 mL) and the combined extracts were dried ($MgSO_4$), filtered and solvent removed under reduced pressure. The residue was purified via Biotage™ Horizon to give **66**.

**Method formation of 67**

Boron tribromide (0.56 mmol) was added dropwise to a solution of **66** (0.28 mmol) in dichloromethane (10.0 mL) at -78 °C. The resulting mixture was stirred for 30 minutes whereupon sodium hydrogen carbonate (10.0 mL of a saturated aqueous solution) was added and the biphasic mixture stirred for 15 minutes until the yellow colour had dissipated. The resulting mixture was stirred at room temperature for 40 minutes, whereupon iodine was added portionwise until the colour due to iodine just persisted and stirring was maintained for 5 minutes. A solution of saturated aqueous sodium thiosulfate was added and the mixture stirred for 30 minutes, diluted with dichloromethane (10.0 mL) and water (20.0 mL). The layers were separated and the aqueous phase extracted with dichloromethane (2 x 20.0 mL). The combined organic extracts were dried over $MgSO_4$, filtered and solvent removed under reduced pressure. The residue was purified *via* Biotage™ Horizon to give **67**.

**Characterization of 62-65, 67 and 69-70**

**(±)-(1S,4S)-5-Allyl-1,2-dibenzyl-7-thia-2,5-diazabicyclo[2.2.1]heptane-3,6-dione 7-sulfide (62)** Pale yellow solid (190 mg, 23%); m.p. 62-64 °C; $\nu_{max}/cm^{-1}$ 1685 (C=O), 1628 (C=C), 734 (C-H), 697 (C-H); δ H (400 MHz, $CDCl_3$) 3.84 (2H, s, C*H*$_2$-Ph), 3.86 – 3.90 (1H, m, NC*H*$_2$CH=CH$_2$), 4.00 – 4.05 (1H, m, NC*H*$_2$CH=CH$_2$), 4.09 (1H, d, *J* 15.0, NC*H*$_2$-Ph), 4.64 (1H, s, C*H*S), 4.75 (1 H, d, *J* 17.1, CH=C*H*$_2$), 5.03 (1H, d, *J* 17.1, CH=C*H*$_2$), 5.22 (1H, d, *J* 15.0, NC*H*$_2$-Ph), 5.55 – 5.67 (1H, m, C*H*=CH$_2$), 6.89 – 6.92 (4H, m, Ar-*H*), 7.36 – 7.42 (6H, m, Ar-*H*); δ C (101 MHz, $CDCl_3$) 35.9 (**C**H$_2$), 46.1 (**C**H$_2$), 48.0 (**C**H$_2$), 55.6 (**C**HS), 59.3 (**C**H=CH$_2$), 114.4 (Ar-**C**-H), 119.5 (CH=**C**H$_2$), 123.9 (Ar-**C**-H), 127.7 (Ar-**C**-H), 128.7 (Ar-**C**-H), 129.7 (Ar-**C**-H), 130.8 (Ar-**C**-H), 134.0 (quaternary **C**), 136.5 (quaternary **C**), 159.4 (quaternary **C**), 163.6 (**C**O), 165.7 (**C**O); *m/z* 397 (100%, $[M+H]^+$); Found $[M+H]^+$ 397.1078, $C_{21}H_{21}N_2O_2S_2$ requires 397.1045.

**(±)-(1S,4S)-1-Allyl-2,5-dibenzyl-7-thia-2,5-diazabicyclo[2.2.1]heptane-3,6-dione 7-sulfide (63)** Pale yellow solid (130 mg, 24%); m.p. 63-65 °C; $\nu_{max}/cm^{-1}$ 1687 (C=O, C=C), 1453 (CH$_2$), 730 (C-H), 697 (C-H); δ H (400 MHz, $CDCl_3$) 3.07 – 3.14 (1H, m, C*H*$_2$CH=CH$_2$), 3.25 – 3.31 (1H, m, C*H*$_2$CH=CH$_2$), 4.53 – 4.58 (1H, m, NC*H*$_2$-Ph), 4.63 – 4.68 (1H, m, NC*H*$_2$-Ph), 4.95 (1H, d, *J* 15.9, NC*H*$_2$-Ph), 5.13 (1H, d, *J* 16.1, NC*H*$_2$-Ph), 5.28 – 5.35 (2H, m, CH=C*H*$_2$), 5.41 (1H, s, C*H*S), 6.16 – 6.20 (1H, m, C*H*=CH$_2$), 7.27 – 7.30 (3H, m, Ar-*H*), 7.32 – 7.36 (4H, m, Ar-*H*), 7.39 – 7.43 (3H, m, Ar-*H*); δ C (101 MHz, $CDCl_3$) 36.4 (**C**H$_2$), 45.4 (**C**H$_2$), 48.7 (**C**H$_2$), 64.2 (**C**HS), 75.2 (quaternary **C**), 120.9 (**C**H$_2$), 127.1 (Ar-**C**-H), 128.0 (Ar-**C**-H), 128.7 (Ar-**C**-H), 128.7 (Ar-**C**-H), 128.9 (Ar-**C**-H), 129.3 (Ar-**C**-H), 131.6 (**C**H=CH$_2$), 134.5 (quaternary **C**), 136.1 (quaternary **C**), 164.6 (**C**O), 165.1 (**C**O); *m/z* 419 (100%, $[M+Na]^+$); Found $[M+Na]^+$ 419.0852, $C_{21}H_{20}N_2O_2S_2Na$ requires 419.0864.

**(±)-(1S,4S)-2-Allyl-1,5-dibenzyl-7-thia-2,5-diazabicyclo[2.2.1]heptane-3,6-dione 7-sulfide (64)** Pale yellow solid (380 mg, 21%); m.p. 63-64 °C; $\nu_{max}/cm^{-1}$ 1672 (C=O), 1627 (C=C), 832 (C-H), 698 (C-H); δ H (400 MHz, $CDCl_3$) 3.84 (2H, s, C*H*$_2$-Ph), 3.87 – 3.91 (2H, m, NC*H*$_2$CH=CH$_2$), 4.04 (1H, d, *J* 6.9, NC*H*$_2$-Ph), 4.65 (1H, s, C*H*S), 4.73 (1H, d, *J* 10.1, CH=C*H*$_2$), 5.04 (1H, d, *J* 10.0, CH=C*H*$_2$), 5.21 (1H, d, *J* 7.1, NC*H*$_2$-Ph), 5.56 – 5.70 (1H, m, C*H*=CH$_2$), 6.85 – 6.90 (2H, m, Ar-*H*), 6.91 – 6.97 (4H, m, Ar-*H*), 7.37 – 7.40 (4H, m, Ar-*H*); δ C (101 MHz, $CDCl_3$) 44.0 (**C**H$_2$), 46.0 (**C**H$_2$), 47.9 (**C**H$_2$), 55.5 (**C**HS), 59.3 (**C**H=CH$_2$), 119.4 (CH=**C**H$_2$), 123.9 (Ar-**C**-H), 127.6 (Ar-**C**-H), 128.7 (Ar-**C**-H), 128.8 (Ar-**C**-H), 129.6 (Ar-**C**-H), 130.7 (Ar-**C**-H), 133.9 (quaternary **C**), 136.4 (quaternary **C**), 159.3 (quaternary **C**), 163.5 (**C**O), 165.6 (**C**O); *m/z* 419 (100%, $[M+Na]^+$); Found $[M+Na]^+$ 419.0973, $C_{21}H_{20}N_2O_2S_2Na$ requires 419.0864.

**(±)-(1S,4S)-1,2-Diallyl-5-benzyl-7-thia-2,5-diazabicyclo[2.2.1]heptane-3,6-dione 7-sulfide (65)** Pale yellow oil (270 mg, 28%); $\nu_{max}/cm^{-1}$ 1674 (C=O), 1609 (C=C), 833 (C-H), 735 (C-H), 701 (C-H); δ H (400 MHz, $CDCl_3$) 3.23 – 3.29 (1H, m, C*H*$_2$CH=CH$_2$), 3.90 – 3.99 (1H, m, C*H*$_2$CH=CH$_2$), 4.41 – 4.48 (2H, m, NC*H*$_2$), 4.82 (1H, d, *J* 14.9, NC*H*$_2$), 5.15 (1H, d, *J* 14.5, NC*H*$_2$), 5.21 (1H, s, C*H*S), 5.22 – 5.27 (2H, m, CH=C*H*$_2$), 5.30 – 5.33 (2H, m, CH=C*H*$_2$), 5.76 – 5.85 (1H, m, C*H*=CH$_2$), 6.07 – 6.12 (1H, m, C*H*=CH$_2$), 7.21 – 7.24 (2H, m, Ar-*H*), 7.27 – 7.31 (3H, m, Ar-*H*); δ C (101 MHz, $CDCl_3$) 36.2 (**C**H$_2$), 45.0 (**C**H$_2$), 48.6 (**C**H$_2$), 64.3 (**C**HS), 75.3 (quaternary **C**), 118.2 (**C**H$_2$), 120.8 (**C**H$_2$), 128.7 (**C**H), 128.7 (Ar-**C**-H), 129.3 (**C**H), 131.7 (Ar-**C**-H), 131.9 (Ar-**C**-H), 134.5 (quaternary **C**), 164.5 (**C**O), 164.7 (**C**O); *m/z* 369 (100%, $[M+Na]^+$); Found $[M+Na]^+$ 369.0726, $C_{17}H_{18}N_2O_2S_2Na$ requires 369.0707.

**(±)-(1S,4S)-1,2,4,5-Tetraallyl-7-thia-2,5-diazabicyclo[2.2.1]heptane-3,6-dione 7-sulfide (67)** White solid (100 mg, 41%); m.p. 180-182 °C; $\nu_{max}/cm^{-1}$ 1639 (C=O, C=C), 1462 (CH$_2$), 749 (CH$_2$); δ H (400 MHz, $CDCl_3$) 3.20 – 3.27 (2H, m, C*H*$_2$CH=CH), 3.28 – 3.36 (2H, m, C*H*$_2$CH=CH), 4.04 (2H, dd, *J* 16.4 & 6.8, NC*H*$_2$), 4.62 (2H, dd, *J* 16.2 & 4.8, NC*H*$_2$), 5.21 – 5.41 (8H, m, CH=C*H*$_2$), 5.89 – 5.94 (2H, m, C*H*=CH$_2$), 6.12 – 6.17 (2H, m, C*H*=CH$_2$); δ C (101 MHz, $CDCl_3$) 36.4 (**C**H$_2$), 45.5 (**C**H$_2$), 74.5 (quaternary **C**), 118.3 (CH=**C**H$_2$), 120.6 (CH=**C**H$_2$), 131.7 (**C**H=CH$_2$), 132.0 (**C**H=CH$_2$), 165.0 (**C**O); *m/z* 337 (100%, $[M+H]^+$); Found $[M+H]^+$ 337.1456, $C_{16}H_{21}N_2O_2S_2$ requires 337.1448.

**(3S,6S)-1,4-Dibenzyl-3,6-dimercaptopiperazine-2,5-dione** (**69**) Prepared as previously described.[18a] m.p. 150-152 °C; IR: $\nu_{max}/cm^{-1}$ 2504, 1661, 1430, 1255; δ H (300 MHz, $CDCl_3$) 2.98 (d, *J* = 7.0 Hz, 2H), 4.08 (d, *J* = 14.5 Hz, 2H), 4.88 (d, *J* = 7 Hz, 2H), 5.17 (d, *J* = 14.5 Hz, 2H), 7.16-7.31 (m, 10H); δ C (75 MHz; $CDCl_3$) 47.9, 56.2, 129.0, 129.1, 129.6, 134.6, 165.1; HRMS (m/z): $[M+Na]^+$ calcd. for $C_{18}H_{18}N_2NaO_2S_2$, 381.0702; found, 381.0700. Consistent with previous report.[18a]

***cis*-1,4-Dibenzyl-3,6-bis(methylthio)piperazine-2,5-dione** (**70**) Sodium borohydride (0.07 g, 1.80 mmol) was added portionwise over 30 minutes to a stirred solution of disulfide (**38**) (0.32 g, 0.90 mmol). Iodomethane (2 mL) in pyridine (3 mL) and methanol (5 mL) were added to the resultant mixture and stirred for 30 minutes where upon a further portion of iodomethane (3 mL) was added and the reaction and stirred for 2 hours. The reaction mixture was poured into water (30 mL) and acidified with dilute aqueous hydrochloric acid (1 M) and extracted with dichloromethane (3 x 50 mL). The combined organic extracts

were dried ($MgSO_4$), filtered and solvent removed under reduced pressure. Purification by flash column chromatography (3: 1, petroleum spirit: ethyl acetate) gave the *cis*-protected dithiodiketopiperazine (**70**) as a colorless solid (280 mg, 80%); m.p. 107-109 ºC; IR: $\nu_{max}/cm^{-1}$ 1674.1, 1429.2, 1169.5; δ H (500 MHz, $CDCl_3$) δ 2.34 (s, 6H), 4.17 (d, *J* = 14.5 Hz, 2H), 4.54 (s, 2H), 5.37 (d, *J* = 14.5 Hz, 2H), 7.40–7.30 (m, 10H); δ C (126 MHz, $CDCl_3$) 16.8, 47.0, 62.2, 128.4, 128.6, 129.1, 134.8, 164.3; HRMS (m/z): $[M]^+$ calcd. for $C_{20}H_{22}N_2NaO_2S_2$, 409.1015; found, 409.1014. Consistent with previous reports.[18a,23c]

**Molecular Modelling**

Molecular modelling was performed using Schrödinger suite 2018-4 and comparative modelling was done using Biovia Discovery Studio Client. Structures of small molecules were prepared using the LigPrep module of Schrodinger Maestro (Schrödinger Inc., New York, NY, USA). The homology model of NCp7 was updated using NMR structure of Zn complex of EIAV NCp1 as template and the model is based on sequence alignment (PDB:2BL6) identity 50%, positive 70%, alignment length 34, E-value 1.88805e-08, resolution: NMR).[8e] The model was constructed using standard settings of Discovery Studio homology modelling protocol. Side chains of the active site residues were further refined using Prime module of Schrodinger. The final model was processed using the protein preparation wizard of Maestro in order to optimize hydrogen bonding network followed by short minimization using 0.3Å rmsd constraint for heavy atoms. Ligand structures were manually docked towards zinc finger motif using our previous models as template and geometry was further refined using "refine protein-ligand complex" functionality embed in Schrodinger suite. Chemical Computing Group's Molecular Operating Environment (MOE v.2018.01) was used to study GRID type of interactions fields to find out if carbonyl oxygen has favorable interaction with zinc.

**DFT studies.**

DFT calculations and Fukui f- functions were calculated using Jaguar module of Schrödinger Suite. Homology model based model compound composition was set up using Maestro software (Schrödinger Inc., New York, NY, USA). The geometry of zinc finger cysteines and histidines were constrained to their initial geometry using Cartesian constraints to connector carbon atoms. The density functional B3LYP of theory and MSV basis set were used for geometry optimizations in the gas phase using Jaguar module of Schrödinger suite.

**Fukui Functions.**

Other than the zinc-finger mimic in the models, structures were geometry optimised using unconstrained gas phase geometry DFT using B3LYP theory and 6-31+G** basis. Fukui functions were computed as single point calculations with default Jaguar keywrods were used (basis=lacvp*+ dftname=b3lyp iacc=1 dconv=5 x $10^{-6}$). The idea behind this is that nucleophilic atoms are those with large, negative values of $f^-$.

**Biology Assays**

**Initial Short Cytotoxicity Assay.**

Crandell Reese feline kidney (CrFK) cells were cultured in 96-well plates (TPP, Trasadingen, Switzerland) at a density of 10,000 cells/well, in complete medium (RPMI 1640 medium (Sigma-Aldrich, Buchs, Switzerland), containing 10% Fetal Calf Serum (FCS) 100 M/mL Glutamine and 1% v/v antibiotic/antimycotic (Ab/Am) (all three, Gibco Life Technologies, Zug, Switzerland). The antiviral compounds were dissolved in 2% DMSO (Sigma-Aldrich, Buchs, Switzerland) to make a 1 mM stock solution. The compounds were 10-fold serially diluted with complete medium. Six dilutions of the compounds (100 µM to 1 nM) were added in triplicate on the CrFK cells (200 µL) and incubated for 24 hours (37 ºC, 5% $CO_2$). The medium was removed and replaced with phenol red free medium and (180 µL) and methylthiazolyldiphenyl-tetrazolium bromide (MTT) (4 mg/mL) (Sigma-Aldrich, Buchs, Switzerland) (20 µL) incubated for 4 hours. The medium was removed by vacuum and the cells were lysed with methanol (200 µL) to reveal a bright purple formazan product. The methanol-formazan absorbance was determined at 570 nM (BioTek Synergy HT plate reader with KC4 software, Cambridge systems) normalized to vehicle treated cells and values expressed as a 50% cytotoxic concentration ($CC_{50}$) as previously described.[25c,40]

**FIV Viral Loading Studies.**

The potential antiviral effect against FIV was tested in a cell culture assay using an IL-2 independent feline FL-4 feline lymphoblastoid cell line. The compounds were added as concentrations ranges in triplicate as above. The cell supernatant (100 µL) was removed, frozen at -20 °C and replaced daily for 7 days. To determine the "long-term" cytotoxicity, on Day 7 the cell culture supernatant was replaced with phenol red free medium (80 µL) and the cells were subjected to the MTT assay (as before). The day 7 cell culture supernatants were centrifuged in a table-top centrifuge (10000 x g) maximal speed for 2 min to pellet cells and debris. Cell culture supernatant of each triplicate were pooled and frozen immediately at -20 ºC until analysis. Total nucleic acids (TNA) were extracted using the MagnaPure LC TNA extraction kit (Roche, Basel, Switzerland) from 200 µL of the pooled supernatants according to manufacturer's instructions. FIV RNA was quantitated by RT-qPCR as described for FIV, using DSMO and untreated cells as controls. Results were expressed as 50% effective concentrations ($EC_{50}$) determined by a sigmoid dose-response curve at 50% inhibition determined by sigmoid dose-response curve fitting using GraphPad Prism version 6.0 (GraphPad Inc., La Jolla, CA, USA) and an RNA standard as previously described.[25c,40]

## Acknowledgments

The authors are grateful to Bloomsbury Colleges - University of London; University College London and Biocenter Finland/DDCB & FCT (grant No. SFRH/BD/65630/2009) for financial support towards the goals of our work. We also thank the Center for Clinical Studies, Vetsuisse Faculty, University of Zurich for logistical support and the CSC-IT Center for Science Ltd. - Finland, for the allocation of computational resources. In addition, we thank the EPSRC UK National Crystallography Service for funding and the collection of the crystallographic data of **36**, **40, 41** & **44**.

**References and notes**

1. A. J. Leslie, K. J. Pfafferott, P. Chetty, R. Draenert, M. M. Addo, M. Feeney, Y. Tang, E. C. Holmes, T. Allen, J. G. Prado, M. Altfeld, C. Brander, C. Dixon, D. Ramduth, P. Jeena, S. A. Thomas, A. St John, T. A. Roach, B. Kupfer, G. Luzzi, A.

Edwards, G. Taylor, H. Lyall, G. Tudor-Williams, V. Novelli, J. Martinez-Picado, P. Kiepiela, B. D. Walker, P. J. R. Goulder, *Nat Med.* **2004**, *10*, 282-289.
2. Report on the Global AIDS Epidemic; UNAIDS: Geneva, Switzerland **2013**
3. (a) N. C. Pedersen, E. W. Ho, M. L. Brown, J. K. Yamamoto, *Science*. **1987**, *235*, 790-793.; (b) T. Hatziioannou, D. T. Evans, *Nat. Rev. Microbiol.* **2012**, *10*, 852-867.; (c) R. B. Meeker, L. Hudson *Vet. Sci.* **2017**, *4*, 14.; (d) Sliva, K. *Expert Opin Drug Discov.* **2015**, *10*, 111-123.
4. (a) Power C. *J Neurovirol.* **2018**, *24*, 220-228.; (b) Willett, B. J.; Hosie, M. J. *Curr Opin Virol*. **2013**, *3*, 670-675.; (c) Miller, M. M.; Fogle, J. E.; Tompkins, M. B. *J Virol.* **2013**, 87, 9373-9378.; (d) Meeker, R. B.; Hudson, L. *Vet. Sci.* **2017**, *4*, 14.
5. Hayes, K. A.; Wilkinson, J. G.; Frick, R.; Francke, S.; Mathes, L. E. *J Acquir Immune Defic Syndr Hum Retrovirol.* **1995**, *9*, 114-122.
6. Clavel, F.; Hance, A. J. N *Engl J Med.* **2004**, *350*, 1023-1035.
7. (a) Rong, L.; Liang, C.; Hsu, M.; Kleiman, L.; Petitjean, P.; de Rocquigny, H.; Roques, B. P.; Wainberg, M. A. *J. Virol.* **1998**, 72, 9353-9358.; (b) Ramboarina, S.; Druillennec, S.; Morellet, N.; Bouaziz, S.; Roques, B. P. *J. Virol.* **2004**, *78*, 6682-6687. (c) Darlix, J. L.; Lapadat-Tapolsky, M.; de Rocquigny, H.; Roques, B. P. *J. Mol. Biol.* **1995**, *254*, 523-537.; (d) Tanchou, V.; Decimo, D.; Péchoux, C.; Lener, D.; Rogemond, V.; Berthoux, L.; Ottmann, M.; Darlix, J. L. *J. Virol.* **1998**, *72*, 4442-4447.; (e) Déméné, H.; Dong, C.; Ottmann, M.; Rouyez, M. C.; Jullian, N.; Morellet, N.; Mely, Y.; Darlix, J. L.; Fournié-Zaluski, M. C.; Saragosti, S.; Roques, B. P. *Biochemistry.* **1994**, *33*, 11707-11716.; (f) Gorelick, R. J.; Gagliardi, T. D.; Bosche, W. J.; Wiltrout, T. A.; Coren, L. V.; Chabot, D. J.; Lifson, J. D.; Henderson, L. E.; Arthur, L. O. *Virology.* **1999**, *256*, 92-104.; (g) Brulé, F.; Marquet, R.; Rong, L.; Wainberg, M. A.; Roques, B. P.; Le Grice, S. F.; Ehresmann, B.; Ehresmann, C. *RNA.* **2002**, *8*, 8-15. (h) Zhang, Y.; Qian, H.; Love, Z.; Barklis, E. *J. Virol.* **1998**, 72, 1782-1789.; (i) Carteau, S.; Batson, S. C.; Poljak, L.; Mouscadet, J. F.; de Rocquigny, H.; Darlix, J. L.; Roques, B. P.; Käs, E.; Auclair, C. *J. Virol.* **1997**, 71, 6225-6229.; (j) Mirambeau, G.; Lyonnais, S.; Coulaud, D.; Hameau, L.; Lafosse, S.; Jeusset, J.; Borde, I.; Reboud-Ravaux, M.; Restle, T.; Gorelick, R. J.; Le Cam, E. *PLoS One.* **2007**, *7*, e669.
8. (a) Morellet, N.; Jullian, N.; De Rocquigny, H.; Maigret, B.; Darlix, J. L.; Roques, B. P. *EMBO J.* **1992**, *11*, 3059-3065.; (b) T. Matsui, Y. Kodera, E. Miyauchi, H. Tanaka, H. Endoh, H. Komatsu, T. Tanaka, T. Kohno, T. Maeda, *Biochem. Biophys. Res. Commun.* **2007**, *358*, 673-678.; (c) M. L. Manrique, M. L. Rauddi, S. A. González, J. L. Affranchino, *J. Virol.* **2004**, *327*, 83-92.; (d) N. Morellet, H. Meudal, S. Bouaziz, B. P. Roques, *Biochem. J.* **2006**, *393*, 725-732.; (e) P. Amodeo, M. A. Castiglione-Morelli, A. Ostuni, G. Battistuzzi, A. Bavoso, *Biochemistry.* **2006**, *45*, 5517-5526.
9. (a) Sancineto, L.; Iraci, N.; Tabarrini, O.; Santi, C. *Drug Discov Today.* **2018**, *23*, 260-271. (b) Iraci, N.; Tabarrini, O.; Santi, C.; Sancineto, L. *Drug Discov Today.* **2018**, *23*, 687-695.
10. Goldschmidt, V.; Miller Jenkins, L. M.; de Rocquigny, H.; Darlix, J.; Mély, Y. *HIV Ther.* **2010**, *4*, 179-198.
11. D. Garg, B. E. Torbett, *Virus Res.* **2014**, *193*, 135-143.
12. (a) Goebel, F. D.; Hemmer, R.; Schmit, J. C.; Bogner, J. R.; de Clercq, E.; Witvrouw, M.; Pannecouque, C.; Valeyev, R.; Vandevelde, M.; Margery, H.; Tassignon, J. P. *AIDS.* **2001**, *15*, 33-45.; (b) Stellbrink H. J. *Antivir. Chem. Chemother.* **2009**, *19*, 189-200.; (c) Hartman, T. L.; Buckheit, R. W. *Mol. Biol. Int.*, **2012**, *2012*, 401965.
13. Sharmeen, L.; McQuade, T.; Heldsinger, A.; Gogliotti, R.; Domagala, J.; Gracheck, S. *Antiviral Res.* **2001**, *49*, 101-114.
14. (a) Rice, W. G.; Schaeffer, C. A.; Harten, B.; Villinger, F.; South, T. L.; Summers, M. F.; Henderson, L. E.; Bess Jr, J. W.; Arthur, L. O.; McDougal, J. S.; Orloff, S. L.; Mendeleyev, J.; Kun, E. *Nature*. **1993**, *361*, 473-475.; (b) Rice, W. G.; Schaeffer, C. A.; Graham, L.; Bu, M.; McDougal, J. S.; Orloff, S. L.; Villinger, F.; Young, M.; Oroszlan, S.; Fesen, M. R. *Proc Natl Acad Sci U S A.* **1993**, *90*, 9721-9724.; (c) Rice, W. G.; Baker, D. C.; Schaeffer, C. A.; Graham, L.; Bu, M.; Terpening, S.; Clanton, D.; Schultz, R.; Bader, J. P.; Buckheit, R. W. Jr.; Field, L.; Singh, P. K.; Turpin, J. A. *Antimicrob Agents Chemother.* **1997**, *41*, 419-426.; (d) Mayasundari, A.; Rice, W. G.; Diminnie, J. B.; Baker, D. C. *Bioorg Med Chem.* **2003**, 11, 3215-3219.; (e) Rice, W. G.; Supko, J. G.; Malspeis, L.; Buckheit, R. W. Jr.; Clanton, D.; Bu, M.; Graham, L.; Schaeffer, C. A.; Turpin, J. A.; Domagala, J.; Gogliotti, R.; Bader, J. P.; Halliday, S. M.; Coren, L.; Sowder, R. C. 2nd.; Arthur, L. O.; Henderson, L. E. *Science.* **1995**, *270*, 1194-1197.; (f) Turpin, J. A.; Song, Y.; Inman, J. K.; Huang, M.; Wallqvist, A.; Maynard, A.; Covell, D. G.; Rice, W. G.; Appella, E. *J Med Chem.* **1999**, *42*, 67-86.
15. Subramanian Vignesh, K.; Deepe, G. S. Jr. *Int J Mol Sci.* **2017**, *18*, E2197.
16. Chen, S. C.; Jeng, K. S.; Lai, M. M. C. *J Virol.* **2017**, *91*, e00842-17.
17. Sekirnik, R.; Rose, N. R.; Thalhammer, A.; Seden, P. T.; Mecinović, J.; Schofield, C. J. *Chem Commun (Camb).* **2009**, *42*, 6376-6378.
18. (a) K. M. Cook, S. T. Hilton, J. Mecinović, W. B. Motherwell, W. D. Figg, C. J. Schofield, *J Biol Chem.* **2009**, *284*, 26831-26838. (b) Burslem, G. M.; Kyle, H. F.; Breeze, A. L.; Edwards, T. A.; Nelson, A.; Warriner, S. L.; Wilson, A. J. *Chembiochem.* **2014**, *15*, 1083-1087.
19. (a) Hurne, A. M.; Chai, C. L.; Moerman, K.; Waring, P. J Biol Chem. 2002, 277, 31631-31638.; (b) Zong, L.; Bartolami, E.; Abegg, D.; Adibekian, A.; Sakai, N.; Matile, S. ACS Cent Sci. 2017, 3, 449-453.; (c) Brea, R. J.; Devaraj, N. K. ACS Cent Sci. 2017, 3, 524-525.
20. (a) Waring, P.; Beaver, J., *Gen. Pharmacol.* **1996**, 27, 1311-1316.; (b) Glister, G. A.; Williams, T. I., *Nature (London, U. K.)* **1944**, 153, 651.; (c) Strunz, G. M.; Kakushima, M.; Stillwell, M. A.; Heissner, C. J., *J. Chem. Soc., Perkin Trans. 1* **1973**, 2600-2602.; (d) Stillwell, M. A.; Magasi, L. P.; Strunz, G. M., *Can. J. Microbiol.* **1974**, *20*, 759-764.; (e) Hauser, D.; Weber, H. P.; Sigg, H. P., *Helv. Chim. Acta* **1970**, *53*, 1061-1073.; (f) Isham, C. R.; Tibodeau, J. D.; Jin, W.; Xu, R.; Timm, M. M.; Bible, K. C., *Blood* **2007**, *109*, 2579-2588.; (g) Seya, H., Nakajima, S., Kawai, K., Udagawa, S., *J. Chem. Soc., Chem. Commun.* **1985**, 657-658.; (h) Onodera, H., Hasegawa, A., Tsumagari, N., Nakai, R., Ogawa, T., Kanda, Y., *Org. Lett.* **2004**, *6*, 4101-4104; (i) Wang, L.; Clive, D. L. J. *Tetrahedron Lett.* **2012**, *53*, 1504-1506.; (j) Nagarajan, R.; Huckstep, L. L.; Lively, D. H.; DeLong, D. C.; Marsh, M. M.; Neuss, N., *J. Amer. Chem. Soc.* **1968**, *90*, 2980-2982; (k) Codelli J. A.; Puchlopek, A. L. A.; Reisman, S. E., *J Am Chem Soc*. **2012**, *134*, 1930-1933.; (l) Neuss, N.; Boeck, L. D.; Brannon, D. R.; Cline, J. C.; DeLong, D. C.; Gorman, M.; Huckstep, L. L.; Lively, D. H.; Mabe, J.; Marsh, M. M.; Molloy, B. B.; Nagarajan, R.; Nelson, J. D.; Stark, W. M., *Antimicrob. Agents Chemother. (Bethesda)* **1968,** *8*, 213-219. (m) Moncrief, J. W. *J. Amer. Chem. Soc.* **1968**, *90*, 6517-6518. (n) Ferezou, J. P.; Riche, C.; Quesneau-Thierry, A.; Pascard-Billy, C.; Barbier, M.; Bousquet, J. F.; Boudart, G., *Nouv. J. Chim.* **1977,** 1, 327-334; (o) Glimelius, K., 1986; de Gruyter: 1986; 629-631.; (p) Synge, R. L. M.; White, E. P., *N. Z. J. Agric. Res.* **1960,** 3, 907-921.; (q) Kishi, Y.; Nakatsuka, S.; Fukuyama, T.; Havel, M. *J Am Chem Soc.* **1973**, *95*, 6493-6495 (u) Gardiner, D. M.; Waring, P.; Howlett, B. J. *Microbiology.* **2005**, *151*(Pt 4), 1021-1032. (v) Bell, M. R.; Johnson, J. R.; Wildi, B. S.; Woodward, R. B. *J. Am. Chem. Soc.* **1958**, *80*, *4*, 1001-1001.; (x) Borthwick, A. D. *Chem Rev.* **2012**, *112*, 3641. 3716. (y) Kim, J.; Ashenhurst, J. A.; Movassaghi, M. *Science.* **2009**, *324*, 238.
21. (a) Öhler, E.; Tataruch, F.; Schmidt, U. *Chem. Ber.* **1972**, *105*, 3658-3661.; (b) Öhler, E.; Poisel, H.; Tataruch, F.; Schmidt, *U. Chem. Ber.* **1972**, *105*, 635-641.; (c) Baumann, E.; Fromm, E. *Ber.* **1891**, *24*, 1441.; (d) Kim, J.; Movassaghi, M. *J. Am. Chem. Soc.* **2010**, *132*, 14376-14278.; (g) Iwasa, E.; Hamashima, Y.; Fujishiro, S.; Hashizume, D.; Sodeoka, M. *Tetrahedron* **2011**, *67*, 6587- 6599.
22. (a) Nicolaou, K. C.; Giguere, D.; Totokotsopoulos, S.; Sun, Y.-P. *Angew. Chem. Int. Ed.* **2012**, *51*, 728-732.
23. (a) Sil, B. C.; Hilton, S. T. *Synlett* **2013**, *24*, 2563-2566.; (b) Szulc, B. R.; Sil, B. C.; Ruiz, A.; Hilton, S. T. Eur. J. Org. Chem. **2015**, *2015*, 7438-7442.; (c) Li, J.; Zhang, Y.; Da Silva Sil Dos Santos, B.; Wang, F.; Ma, Y.; Perez, C.; Yang, Y.; Peng, J.; Cohen, S. M.; Chou, T. F.; Hilton, S. T.; Deshaies, R. J. *Cell Chem Biol.* **2018**, *25*, 1350-1358.
24. Crandell, R. A.; Fabricant, C. G.; Nelson-Rees, Walter A. *In Vitro* **1973**, *9*, 176-185.
25. (a) Asquith, C. R. M., Meli, M. L., Konstantinova, L. S., Laitinen, T., Peräkylä, M., Poso, A., Rakitin, O. A., Allenspach, K., Hofmann-Lehmann, R., Hilton, S. T. *Bioorg. Med. Chem. Lett.* **2014**, *24*, 2640-2644.; (b) Asquith, C. R. M., Meli, M. L., Konstantinova, L. S., Laitinen, T., Poso, A., Rakitin, O. A., Hofmann-Lehmann, R., Allenspach, K., Hilton, S. T. *Bioorg. Med. Chem. Lett.* **2015**, *25*, 1352-1355.; (c) Asquith, C. R. M.,

Konstantinova, L. S., Meli, M. L., Laitinen, T., Poso, A., Rakitin, O. A., Hofmann-Lehmann, R., Hilton, S. T. *ChemMedChem* **2016**, *11*, 2119-2126.; (d) Asquith, C. R. M., Laitinen, T., Konstantinova, L. S., Poso, A., Rakitin, O. A., Hofmann-Lehmann, R., Hilton, S. T. *ChemMedChem.* **2019**, *14*, 454-461.; (e) Asquith, C. R. M., Meili, T., Laitinen, T., Baranovsky, I. V., Konstantinova, L. S., Poso, A., Rakitin, O. A., Hofmann-Lehmann, R. *Bioorg. Med. Chem. Lett.* **2019**, *29*, 1765-1768.

26. Yamamoto, J. K.; Ackley, C. D.; Zochlinski, H.; Louie, H.; Pembroke, E.; Torten, M.; Hansen, H.; Munn, R.; Okuda, T. *Intervirology.* **1991**, *32*, 361-375.
27. Klein, D.; Leutenegger, C. M.; Bahula, C.; Gold, P.; Hofmann-Lehmann, R.; Salmons, B.; Lutz, H.; Gunzburg, W. H. *J. Acquired Immune Defic. Syndr.* **2001**, *26*, 8-20.
28. Bisset, L. R.; Lutz, H.; Böni, J.; Hofmann-Lehmann, R.; Lüthy, R.; Schepbach, J. *Antiviral Res.* **2002**, 53, 35-45.
29. Summa, V.; Petrocchi, A.; Bonelli, F.; Crescenzi, B.; Donghi, M.; Ferrara, M.; Fiore, F.; Gardelli, C.; Gonzalez Paz, O.; Hazuda, D. J.; Jones, P.; Kinzel, O.; Laufer, R.; Monteagudo, E.; Muraglia, E.; Nizi, E.; Orvieto, F.; Pace, P.; Pescatore, G.; Scarpelli, R.; Stillmock, K.; Witmer, M. V.; Rowley, M. *J Med Chem.* **2008**, *51*, 5843-5855.
30. (a) Jain, S.; Patel, N.; Lin, S. *Drug Dev Ind Pharm.* **2015**, *41*, 875-887. (b) K. A, Chu; S. H. Yalkowsky, *Int J Pharm.* **2009**, *373*, 24-40. (c) Savjani, K. T.; Gajjar, A. K.; Savjani, J. K. *ISRN Pharm.* **2012**, *2012*, 195727.
31. Bochevarov, A. D.; Harder, E.; Hughes, T. F.; Greenwood, J. R.; Braden, D. A.; Philipp, D. M.; Rinaldo, D.; Halls, M. D.; Zhang, J.; Friesner, R. A. *Int. J. Quan. Chem.* **2013**, *113*, 2110-2142.
32. (a) P. W. Ayers, R. G. Parr, *J. Am. Chem. Soc.* **2001**, *123*, 2007-2017. (b) P. W. Ayers, R. C. Morrison, R. K. Roy, *J. Chem. Phys.* **2002**, *116*, 8731.
33. A summary of the crystallographic data collection parameters and refinement details for **36**, **40**, **41** and **44** are presented in the supporting information. Anisotropic parameters, bond lengths and (torsion) angles for these structures are available from the CIF files which have been deposited with the Cambridge Crystallographic Data Centre and given the following deposition numbers, 1847904 (**36**), 1847906 (**40**). 1922518 (**41**) and 1847907 (**44**). These data can be obtained free of charge from The Cambridge Crystallographic Data Centre *via* www.ccdc.cam.ac.uk/data_request/cif.
34. The Cambridge Structural Database v.5.39 (Nov 2017). C. R. Groom, I. J. Bruno, M. P. Lightfoot, S. C. Ward, *Acta Cryst.*, **2016**, B72, 171-179.
35. Cappel, D.; Sherman, W.; Beuming, T. *Curr Top Med Chem.* **2017**, *17*, 2586-2598.
36. (a) Loo, J. A,; Holler, T. P.; Sanchez, J.; Gogliotti, R.; Maloney, L.; Reily, M. D. *J Med Chem.* **1996**, *39*, 4313-4320.; (b) J. C. Woodcock, W. Henderson, C. O. Miles *J. Inorg. Biochem.* **2001**, *85*, 187-199.; (c) J. C. Woodcock, W. Henderson, C. O. Miles, B. K. Nicholson *J. Inorg. Biochem.* **2001**, *84*, 225-232.
37. S. Fujishiro, K. Dodo, E. Iwasa, Y. Teng, Y. Sohtome, Y. Hamashima, A. Ito, M. Yoshida, M. Sodeoka, *Bioorg Med Chem Lett.* **2013**, *23*, 733-736.
38. W. C. Still, M. Kahn, A. Mitra, *J. Org. Chem.* **1978,** *43*, 2923-2925.
39. T. Fukuyama, S.-I. Nakatsuka, Y. Kishi, *Tetrahedron* **1981**, *37*, 2045-2078.
40. P. W. Sylvester, *Methods Mol. Biol.* **2011**, *716*, 157-168.